

PCT

WORLD INTELLECTUAL PROPERTY ORGANIZATION
International Bureau



INTERNATIONAL APPLICATION PUBLISHED UNDER THE PATENT COOPERATION TREATY (PCT)

(51) International Patent Classification 6 : G01R 33/28	A1	(11) International Publication Number: WO 97/37239 (43) International Publication Date: 9 October 1997 (09.10.97)
(21) International Application Number: PCT/US97/05166		H, 1131 6th Street, Albany, CA 94710 (US). PIETRASS, Tanja [DE/US]; 906 School of Mines Road 12, Socorro, NM 87801 (US).
(22) International Filing Date: 28 March 1997 (28.03.97)		(74) Agents: GARRETT-WACKOWSKI, Eugenia et al.; Townsend and Townsend and Crew L.L.P., 8th floor, Two Embar- cadero Center, San Francisco, CA 94111 (US).
(30) Priority Data: 60/014,321 29 March 1996 (29.03.96) US		(81) Designated States: AL, AM, AT, AU, AZ, BA, BB, BG, BR, BY, CA, CH, CN, CU, CZ, DE, DK, EE, ES, FI, GB, GE, GH, HU, IL, IS, JP, KE, KG, KP, KR, KZ, LC, LK, LR, LS, LT, LU, LV, MD, MG, MK, MN, MW, MX, NO, NZ, PL, PT, RO, RU, SD, SE, SG, SI, SK, TJ, TM, TR, TT, UA, UG, US, UZ, VN, YU, ARIPO patent (GH, KE, LS, MW, SD, SZ, UG), Eurasian patent (AM, AZ, BY, KG, KZ, MD, RU, TJ, TM), European patent (AT, BE, CH, DE, DK, ES, FI, FR, GB, GR, IE, IT, LU, MC, NL, PT, SE), OAPI patent (BF, BJ, CF, CG, CI, CM, GA, GN, ML, MR, NE, SN, TD, TG).
(71) Applicant (<i>for all designated States except US</i>): LAWRENCE BERKELEY NATIONAL LABORATORY [US/US]; 1 Cy- clotron Road, Mailstop 90-1121, Berkeley, CA 94720 (US).		Published <i>With international search report.</i> <i>Before the expiration of the time limit for amending the claims and to be republished in the event of the receipt of amendments.</i>
(72) Inventors; and (75) Inventors/Applicants (<i>for US only</i>): PINES, Alexander [US/US]; 710 Keeler Street, Berkeley, CA 94708 (US). BUDINGER, Thomas [US/US]; 966 Euclid, Berkeley, CA 94708 (US). NAVON, Gil [IL/IL]; 24 Hameiri Street, 52651 Ramat Gan (IL). SONG, Yi-Qiao [CN/US]; 1671 Arch Street #1, Berkeley, CA 94709 (US). APPELT, Stephan [DE/US]; Apartment I, 2741 Dwight Avenue, Berkeley, CA 94704 (US). BIFONE, Angelo [IT/IT]; Cam- pano, 52, Via San Pantaleo, I-00149 Rome (IT). TAYLOR, Rebecca [US/US]; 2525 Benvenue Avenue #2, Berkeley, CA 94704 (US). GOODSON, Boyd [US/US]; 2141 Oregon Street #1, Berkeley, CA 94705 (US). SEYDOUX, Roberto [CH/US]; Apartment 5, 3100 College Avenue, Berkeley, CA 94702 (US). ROOM, Toomas [EE/US]; Apartment		

(54) Title: ENHANCEMENT OF NMR AND MRI IN THE PRESENCE OF HYPERPOLARIZED NOBLE GASES

(57) Abstract

The present invention relates generally to nuclear magnetic resonance (NMR) techniques for both spectroscopy and imaging. More particularly, the present invention relates to methods in which hyperpolarized noble gases (e.g., Xe and He) are used to enhance and improve NMR and MRI. Additionally, the hyperpolarized gas solutions of the invention are useful both *in vitro* and *in vivo* to study the dynamics or structure of a system. When used with biological systems, either *in vivo* or *in vitro*, it is within the scope of the invention to target the hyperpolarized gas and deliver it to specific regions within the system.

BEST AVAILABLE COPY

FOR THE PURPOSES OF INFORMATION ONLY

Codes used to identify States party to the PCT on the front pages of pamphlets publishing international applications under the PCT.

AL	Albania	ES	Spain	LS	Lesotho	SI	Slovenia
AM	Armenia	FI	Finland	LT	Lithuania	SK	Slovakia
AT	Austria	FR	France	LU	Luxembourg	SN	Senegal
AU	Australia	GA	Gabon	LV	Latvia	SZ	Swaziland
AZ	Azerbaijan	GB	United Kingdom	MC	Monaco	TD	Chad
BA	Bosnia and Herzegovina	GE	Georgia	MD	Republic of Moldova	TG	Togo
BB	Barbados	GH	Ghana	MG	Madagascar	TJ	Tajikistan
BE	Belgium	GN	Guinea	MK	The former Yugoslav Republic of Macedonia	TM	Turkmenistan
BF	Burkina Faso	GR	Greece	ML	Mali	TR	Turkey
BG	Bulgaria	HU	Hungary	MN	Mongolia	TT	Trinidad and Tobago
BJ	Benin	IE	Ireland	MR	Mauritania	UA	Ukraine
BR	Brazil	IL	Israel	MW	Malawi	UG	Uganda
BY	Belarus	IS	Iceland	MX	Mexico	US	United States of America
CA	Canada	IT	Italy	NE	Niger	UZ	Uzbekistan
CF	Central African Republic	JP	Japan	NL	Netherlands	VN	Viet Nam.
CG	Congo	KE	Kenya	NO	Norway	YU	Yugoslavia
CH	Switzerland	KG	Kyrgyzstan	NZ	New Zealand	ZW	Zimbabwe
CI	Côte d'Ivoire	KP	Democratic People's Republic of Korea	PL	Poland		
CM	Cameroon	KR	Republic of Korea	PT	Portugal		
CN	China	KZ	Kazakhstan	RO	Romania		
CU	Cuba	LC	Saint Lucia	RU	Russian Federation		
CZ	Czech Republic	LI	Liechtenstein	SD	Sudan		
DE	Germany	LK	Sri Lanka	SE	Sweden		
DK	Denmark	LR	Liberia	SG	Singapore		

***ENHANCEMENT OF NMR AND MRI
IN THE PRESENCE OF
HYPERPOLARIZED NOBLE GASES***

FIELD OF THE INVENTION

The present invention relates generally to nuclear magnetic resonance (NMR) techniques for both spectroscopy and imaging. More particularly, the present invention relates to the use of hyperpolarized noble gases (e.g., Xe and He) to enhance and improve NMR and MRI.

BACKGROUND OF THE INVENTION

Nuclear magnetic resonance (NMR) is an established technique for both spectroscopy and imaging. NMR spectroscopy is one of the most powerful methods available for determining primary structure, conformation and local dynamic properties of molecules in liquid, solid and even gas phases. As a whole-body imaging technique, Magnetic Resonance Imaging (MRI) affords images possessing such superb soft tissue resolution that MRI is the modality of choice in many clinical settings. MRI can produce images which allow the clinician to distinguish between a pathological condition and healthy tissue. For example, MR images clearly differentiate tumors from the surrounding tissue. Further, using MRI it is possible to image specific regions within the organism and to obtain anatomical (morphology and pathology) and/or functional information about various processes including blood flow and tissue perfusion. Functional imaging of the brain is now also well documented.

The structural and functional information available through MRI is complemented by whole-body NMR spectroscopy. NMR spectroscopic studies on organisms provides a means to probe the chemical processes occurring in the tissue under study. For example, the location and quantity of intrinsic NMR spectroscopic markers such as lactate and citrate can be studied to gain insight into the chemical processes underlying a disease state (Kurhanewicz, J., *et al.*, *Urology* 45: 459-466 (1995)). NMR spectroscopy can also be used to observe the effects of administered drugs on the biochemistry of the organism or the changes in the drug which occur following its administration (Maxwell, R.J., *Cancer Surv.* 17: 415-423 (1993)). Efforts to improve the information yield from MRI and NMR spectroscopy through increased sensitivity or the use of appropriately designed extrinsic probes have been ongoing since the inception of these techniques.

Sensitivity poses a persistent challenge to the use of NMR, both in imaging and spectroscopy. In proton MRI, contrast is primarily governed by the quantity of protons in a tissue and the intrinsic relaxation times of those protons (i.e., T_1 and T_2). Adjacent tissues which are histologically distinct yet magnetically similar appear isointense on an MR image. As the proton content of a tissue is not a readily manipulable parameter, the approach taken to provide distinction between magnetically similar tissues is the introduction into the biological system of a paramagnetic pharmaceutical (*i.e.*, contrast enhancing agent) such as Gd(DTPA) (Niendorf, H.P., *et al.*, *Eur. J. Radiol.*, 13: 15 (1991)). Interaction between the proton nuclei and the unpaired spins on the Gd^{+3} ion dramatically decrease the proton relaxation times causing an increase in tissue intensity at the site of interaction. Gd(DTPA) and analogous agents are small molecular agents which remain largely confined to the extracellular compartment and do not readily cross the intact blood-brain barrier. Thus, these agents are of little use in functional brain imaging.

Similar to MRI, NMR spectroscopic studies generally rely on detecting NMR active nuclei which are present in their natural abundance (*e.g.*, 1H , ^{31}P , ^{13}C) (Sapega, A.A., *et al.*, *Med. Sci. Sports Exerc.*, 25: 656-666 (1993)). Additionally, the chemical species under observation must be spectroscopically distinguishable from the other compounds within the window of observation. Thus, sensitivity in NMR spectroscopy is a function of both the abundance and the spectral characteristics of the molecule(s) desired to be studied. The range of NMR spectroscopic studies has been somewhat expanded by the application of exogenous probes which contain NMR active nuclei, for example ^{19}F (Aiken, N.R., *et al.*, *Biochim. Biophys. Acta*, 1270: 52-57 (1995)).

Noble gases are of interest as tracers and probes for MRI and NMR spectroscopy (Middleton, H., *et al.*, *Magn. Res. Med.* 33: 271 (1995)), however, the sensitivity of MRI and NMR spectroscopy for these molecules is relatively low. A factor which contributes to the lack of sensitivity of these techniques for the noble gases is that the spin polarization, or net magnetic moment, of the noble gas sample is low. For example, a typical molecule at thermal equilibrium at room temperature has an excess of spins in one direction along an imposed magnetic field relative to those in the opposite direction of generally less than 1 in 10^5 . Lower temperatures and higher fields, to the extent that these can be imposed, provide only limited benefit. Alternative approaches rely on disrupting the equilibrium magnetization by forcing molecules in the sample into a polarized state. Two methods known in the art for enhancing the spin polarization of a population of nuclei are dynamic nuclear polarization and optical pumping.

Dynamic nuclear polarization, originally applied to metals, arises from the cross relaxation between coupled spins. The phenomenon is known as the Overhauser Effect, with early disclosures by Overhauser and others (Overhauser, A.W., "Polarization

of nuclei in metals," *Phys. Rev.* **92**(2): 411-415 (1953), Solomon, I., "Relaxation processes in a system of two Spins," *Phys. Rev.* **99**(2): 559-565 (1955), and Carver, T.R., *et al.*, "Experimental verification of the Overhauser nuclear polarization effect," *Phys. Rev.* **102**(4): 975-980 (1956)). The Nuclear Overhauser Effect between nuclear spins is widely used to determine interatomic distances in NMR studies of molecules in solution.

Optical pumping is a method for enhancing the spin polarization of gases which consists of irradiating an alkali metal, in the presence of a noble gas, with circularly polarized light. The hyperpolarized gases that result have been used for NMR studies of surfaces and imaging void spaces and surfaces. Examples are the enhanced surface NMR of hyperpolarized ^{129}Xe , as described by Raftery, D., *et al.*, *Phys. Rev. Lett.* **66**: 584 (1991); signal enhancement of proton and ^{13}C NMR by thermal mixing from hyperpolarized ^{129}Xe , as described by Driehuys, B., *et al.*, *Phys. Lett. A* **184**: 88-92 (1993), and Bowers, C.R., *et al.*, *Chem. Phys. Lett.* **205**: 168 (1993), and by Hartmann-Hahn cross-polarization, as described by Long, H.W., *et al.*, *J. Am. Chem. Soc.* **115**: 8491 (1993); and enhanced MRI of void spaces in organisms (such as the lung) and other materials, as described by Albert, M.S., *et al.*, *Nature* **370**: 199-201 (1994), and Song, Y.-Q., *et al.*, *J. Magn. Reson. A* **115**: 127-130 (1995).

Although hyperpolarized noble gases have proven useful as probes in the study of the air spaces in lungs, the effectiveness or sensitivity of these methods is somewhat compromised for biological materials and organs, such as blood and the parts of the body that are accessible only through the blood. During its residence time in the blood, the hyperpolarized gas is diluted considerably and the delay in transferring the gas from the lung space to the blood consumes much of the time (e.g., T_1) required for the polarized gas to return to its non-hyperpolarized state. Further complicating the situation, the penetration of the hyperpolarized gas into the interior of red blood cells dramatically reduces the T_1 of the hyperpolarized gas and thus, sorely attenuates the temporal range over which the gas can serve as an effective probe.

A considerable advance in both MRI and NMR spectroscopy could be achieved by the introduction of a versatile hyperpolarized noble gas-based NMR active tracer which could also function as a contrast enhancing agent or otherwise affect, in a spectroscopically discernable manner, sample molecules to which the probe is proximate. Among other applications, such an agent would be useful in conjunction with functional imaging of the brain and also to probe the dynamics of exchange between the intracellular and extracellular compartments of various tissues. Of even more profound significance would be a means of delivering the tracer, either through the blood or via direct injection into the tissue of interest, which maintains the hyperpolarization of the gas during the delivery process and through the imaging or spectroscopic experiment. Quite surprisingly, the instant invention provides both such a tracer and delivery method.

SUMMARY OF THE INVENTION

The present invention provides methods for using hyperpolarized noble gases in conjunction with NMR spectroscopy and MRI. The noble gases are useful both as tracers, which are themselves detected, and also as agents which affect the magnetic properties of other nuclei present in a sample.

Thus, in a first aspect, the present invention provides a method for analyzing a sample containing an NMR active nucleus, the method comprising:

- (a) contacting the sample with a hyperpolarized noble gas;
- (b) scanning the sample by nuclear magnetic resonance spectroscopy, magnetic resonance imaging, or both nuclear magnetic resonance spectroscopy and magnetic resonance imaging;
- (c) detecting the NMR active nucleus, wherein the NMR active nucleus is a nucleus other than a noble gas.

In another aspect, the present invention provides a method for analyzing a sample which comprises: (a) combining a hyperpolarized noble gas with a fluid to form a mixture; (b) contacting the sample with the mixture; and (c) scanning the sample, the noble gas or both the sample and the noble gas by nuclear magnetic resonance spectroscopy, magnetic resonance imaging, or both nuclear magnetic resonance spectroscopy and magnetic resonance imaging.

In a further aspect, the invention provides a pharmaceutical composition which comprises a hyperpolarized noble gas dissolved in a physiologically compatible liquid carrier.

In yet another aspect, the present invention provides a method for studying a property of a noble gas in a tissue. This method of the invention comprises:

(a) hyperpolarizing a noble gas; (b) dissolving the hyperpolarized noble gas in a physiologically compatible liquid carrier to form a mixture; (c) contacting the tissue with the mixture from (b); and (d) scanning the tissue by nuclear magnetic resonance, magnetic resonance imaging, or both, whereby the property of the noble gas in the tissue is studied.

In a further aspect, the invention provides a method for enhancing the relaxation time of a hyperpolarized noble gas in contact with a physiological fluid. This method comprises: (a) forming a hyperpolarized noble gas intermediate solution by dissolving the hyperpolarized noble gas in a fluid in which the relaxation time of the noble gas is longer than the relaxation time of the noble gas in the physiological fluid; and (b) contacting the physiological fluid with the intermediate solution.

In yet a further aspect, the present invention provides a method for measuring a signal transferred from at least one hyperpolarized noble gas atom to at least

one non-noble gas NMR active nucleus, comprising: (a) contacting a non-noble gas NMR active nucleus with a hyperpolarized noble gas atom; (b) applying radiofrequency energy to the non-noble gas NMR active nucleus in a magnetic field; and (c) measuring the signal transferred from the hyperpolarized noble gas atom to the non-noble gas NMR active nucleus using nuclear magnetic resonance spectroscopy, magnetic resonance imaging, or both.

In a still further aspect, the invention provides a pulse sequence for heteronuclear difference spin polarization induced nuclear Overhauser effect (SPINOE) NMR of a system comprising at least one hyperpolarized noble gas atom and at least one non-noble gas NMR active nucleus, comprising: (a) at least one non-noble gas NMR active nucleus $\pi/2$ pulse; (b) a non-noble gas NMR active nucleus π pulse applied simultaneously with application of a noble gas π pulse; and (c) a non-noble gas NMR active nucleus $\pi/2$ pulse.

In an additional aspect, the invention provides an apparatus for preparing a solution of a hyperpolarized noble gas in a fluid, the apparatus comprising:

a vessel for receiving the fluid;
a reservoir for receiving the hyperpolarized noble gas, the reservoir communicating through a first shutoff valve with the vessel, the reservoir being shaped to allow the reservoir to be cooled independently of the vessel;
a gas inlet port communicating through a second shutoff valve with the reservoir; and
a means for withdrawing the fluid from the vessel independently of the first and second shutoff valve.

Other features, objects and advantages of the invention and its preferred embodiments will become apparent from the detailed description which follows.

BRIEF DESCRIPTION OF THE DRAWINGS

FIG. 1. A schematic is set forth of the experimental protocol used.

Eighty percent of isotopically enriched ^{129}Xe is polarized via spin exchange with optically pumped rubidium atoms using previously described techniques. The xenon is frozen at liquid nitrogen temperature in a sidearm of a sample tube in high magnetic field provided by a permanent magnet. The xenon is then brought to the gas phase by warming and admitted to the solution.

FIG. 2. ^{129}Xe NMR spectrum of a solution of ^{129}Xe in D_2O

FIGS. 3A and 3B. Conventional and optically polarized ^{129}Xe NMR spectra of xenon in blood acquired after injecting 1 cc of xenon/water mixture into 1 cc of concentrated red blood cells are set forth.

FIG. 4. The time dependence of the integrals of the two peaks in a typical ^{129}Xe NMR of ^{129}Xe in blood is set forth.

FIGS. 5A and 5B. Intrinsic exchange of xenon between the extracellular and intracellular compartments of blood. FIG. 5A shows the initial equilibrium spectrum and the time dependent spectra following the selective inversion. FIG. 5B shows the time dependence of the signal intensities.

FIGS. 6A and 6B. Optically pumped ^{129}Xe spectrum of xenon delivered to blood in the INTRALIPID® solution is provided (A). 2-dimensional ^{129}Xe MR image laser-polarized xenon in blood/INTRALIPID® (A, inset). A ^{129}Xe spectrum acquired after mixing the xenon/FLUOSOL® solution in whole blood (B). Compressed ^{129}Xe NMR spectrum of xenon/FLUOSOL® solution in whole blood (B, inset).

FIG. 7. Two-dimensional magnetic resonance image of ^{129}Xe dissolved in fresh human blood taken immediately after the blood is mixed with the saline saturated by hyperpolarized xenon. The 128x64 images were taken by the Echo Planar Imaging (EPI) method on a Quest 4300 spectrometer. The diameter of the sample tube is 10 mm, and the solution occupies a region of length of 20 mm.

FIG. 8. Time dependence of the hyperpolarized ^{129}Xe NMR signal observed in benzene solution after being contacted with hyperpolarized xenon. The main figure shows the data for partially deuterated benzene (25 % $\text{C}_6\text{D}_5\text{H}$, 75% C_6D_6); the inset shows the data for normal benzene (C_6H_6). In the experiments represented by open circles, xenon was admitted into benzene by opening the xenon reservoir; the initial rise in signal represents the penetration of xenon into the solvent. In the experiment represented by closed circles, the xenon was mixed with the benzene by shaking the sample after opening the xenon reservoir, so as to produce a uniform saturated solution. ^{129}Xe spin polarization was enhanced by optical pumping using circularly polarized light at 794.7 nm. Typically, 4×10^4 moles of enriched ^{129}Xe were used in one experiment. The difference in the ^{129}Xe signal between benzene and deuterated benzene demonstrates the effect of magnetic dipolar coupling between ^1H and ^{129}Xe spins on the relaxation of the ^{129}Xe . For the initial NOE experiments, the partially deuterated liquids were used in order to favor the effects of cross-relaxation over those contributing to ^1H auto-relaxation. ^{129}Xe NMR was performed at 51 MHz on a Quest 4300 spectrometer using a home-built probe and a tipping angle of 3°.

FIG. 9. Time dependence of the ^1H NMR signal observed after exposure of partially deuterated benzene (25% $\text{C}_6\text{D}_5\text{H}$, 75% C_6D_6) to hyperpolarized ^{129}Xe . The sample was exposed to xenon at zero magnetic field and was then inserted into the NMR probe within a few seconds. The initial rise of the ^1H signal is due to spin-lattice relaxation. The ^1H NMR signal exhibits a positive (O) or negative (◊) NOE depending on the sign of the ^{129}Xe polarization. From the variation of the ^1H signal in the presence of

unpolarized xenon (\square), the $^1\text{H} T_1$ of the benzene-xenon solution is determined to be ~ 160 s. Inset: Time dependence of the ^1H NMR signal after polarized ^{129}Xe was dissolved in partially deuterated benzene. Prior to admitting the xenon, the sample was placed in the NMR magnet for approximately 10 minutes to allow thermal equilibration of the ^1H magnetization. After the xenon reservoir was opened, the sample was then shaken to ensure efficient mixing of the xenon and benzene. The smooth lines represent a fit to the time dependent solution (J. H. Noggle, R. E. Schirmer, *The Nuclear Overhauser Effect: Chemical Applications* (Academic Press, New York-London-Toronto-Sidney-San Francisco, 1971)) of Eq. 1.

$$I(t) = a + b(e^{-t/\tau_1} - e^{-t/\tau_2}) \quad (1)$$

yielding time constants of 120s and 1050s (\bullet), and 140s and 1020s (\blacklozenge). ^1H NMR was performed at 185 MHz using a home-built probe and a tipping angle of 3° .

FIG. 10. Time-resolved, two-dimensional magnetic resonance images of ^{129}Xe dissolved in benzene, taken after the exposure of the benzene to hyperpolarized ^{129}Xe . A Xe concentration gradient exists immediately after the Xe is admitted, evolving with time to a more uniform solution. The 64 pixel by 128 pixel images were taken by the fast low-angle shot (FLASH) imaging method on a Quest 4300 spectrometer, with a tipping angle of 3° for each of the 64 signal acquisitions. The frequency-encoding gradient was 3.5 G/mm. The step size of the phase-encoding gradient pulses, which were 500 μs long, was 0.063 G/mm. The diameter of the sample tube is 7 mm, and the solution occupies a region of length 15 mm.

FIG. 11. Time-resolved distribution of ^{129}Xe magnetization in partially deuterated benzene from MRI projection along the tube axis (z). The sample was not shaken after xenon was admitted to the benzene in order to prevent a uniform initial concentration. In the first image taken 47s after the admission of the xenon gas to the solution three regions may be distinguished. The intensity above the solution level (above 18 mm) arises from ^{129}Xe in the gas phase which is displaced from the dissolved ^{129}Xe signal due to its different chemical shift. The decrease of the gas signal above 21 mm along the z axis is due to the declining NMR sensitivity beyond the radiofrequency coil, represented by circles in the schematic. The signal maximum at a position of 15.2 mm corresponds to the top of the solution, arising from xenon diffusing into the solution from the gas phase. The signal maximum at about 1.3 mm corresponds to the lower end of the tube. Thus, xenon accumulates at the bottom of the sample tube first and a discernible xenon concentration gradient persists for up to 5 minutes. The concentration gradient results from natural convection due to density differences between the xenon solution and that of pure benzene, progressing ultimately to a uniform saturated xenon solution. The imaging field gradient was 2.6 G/mm.

FIG. 12. Two-dimensional magnetic resonance images of the NOE enhanced ¹H signals at 2 and 6 minutes after hyperpolarized xenon was admitted to the sample tube containing normal benzene. The enhancement images were obtained by subtracting the equilibrium image shown, which is the average of four images taken after 25 minutes. The intensity scale in the difference images has been magnified 8-fold for clarity. The maximum NOE enhancement in the 2 minute image is 0.05; that in the 6 minute image is 0.12. A perceptible gradient of the enhanced ¹H signal is observed in the 2 minute image, corresponding to the observed gradient in the xenon concentration and the enhancement is found to be uniform in the 6 minute image when the xenon concentration gradient is diminished. The negative region in the 2 minute image could be caused by expansion of the liquid phase as xenon dissolves. The images were taken by the Echo Planar Imaging method (Mansfield, P., *J. Phys. C* **10**, L55 (1977)) in 24 ms. The frequency-encoding gradient was 3.15 G/mm; the phase-encoding gradient pulses were 0.14 G/mm and 50 μ s long. The image dimension was 128 \times 32, and the image was zero-filled to 256 \times 256 in data processing. The skew of the image is due to the inhomogeneity of the static magnetic field.

FIG. 13. Schematic diagram of the pulse sequence used to obtain heteronuclear difference SPINOE spectra. The proton magnetization is saturated first by a series of $\pi/2$ pulses and a z-axis magnetic field gradient is applied in between the pulses to dephase the transverse components of the magnetization for optimal saturation. The π pulses help to reduce the growth of proton signal due to spin-lattice relaxations. A π pulse is also applied to the ¹²⁹Xe resonance at the same time of the proton π pulses so that the ¹²⁹Xe magnetization is inverted in synchronization with the proton magnetization. This synchronization ensures that the SPINOE signals will be accumulated during the entire mixing time. Both proton and xenon π pulses are adiabatic pulses BIR4 of 1 ms in duration.

FIG. 14A and 14B. (A) Proton spectra of 0.1 M *p*-nitrotoluene solution in perdeuterated benzene at thermal equilibrium; (B) SPINOE proton spectra of 0.1 M *p*-nitrotoluene solution in perdeuterated benzene with positive and negative ¹²⁹Xe spin polarization. The total mixing time is 2.1 s.

FIG. 15. Proton spectra of 0.05 M α -cyclodextrin solution in perdeuterated DMSO (dimethyl sulfoxide) at thermal equilibrium;

FIG. 16. SPINOE spectrum of α -cyclodextrin in the presence of negatively polarized ¹²⁹Xe.

FIG. 17. SPINOE spectrum of α -cyclodextrin in the presence of positively polarized ¹²⁹Xe. The positive ¹²⁹Xe polarization is defined to be along the thermal equilibrium polarization. The total mixing time is 1 s and two signals were acquired for each spectrum.

FIG. 18. Schematic diagram showing the process used for *in vivo* imaging of hyperpolarized ^{129}Xe in the rat.

FIG. 19. A ^{129}Xe xenon spectrum representing an average of the sixth through the twelfth scan in a series of ^{129}Xe spectra taken over the thorax and abdomen areas following intravenous injection of a xenon/INTRALIPID® solution in the rat.

FIG. 20. Schematic diagram of the ^{129}Xe imaging experiment showing the timing of and relationship between the excitation pulse, slice selection pulse, first and second gradients and signal detection.

FIG. 21. Two dimensional ^{129}Xe images taken at intervals of approximately 7 seconds. The images depict the ^{129}Xe signal intensity in the upper part of the rat's hind leg.

FIG. 22. A representation of one possible apparatus to accomplish the mixing of a hyperpolarized noble gas with a fluid as contemplated by this invention. The apparatus has four main subcomponents: a vessel for receiving the fluid 10, a noble gas reservoir 20, a gas inlet port 40, and a means to remove the liquid from the vessel 60. The reservoir and the vessel are connected by means of a shutoff valve 30. Similarly, the reservoir and the gas inlet port are connected via a shutoff valve 50.

DETAILED DESCRIPTION OF THE INVENTION AND PREFERRED EMBODIMENTS

It has been discovered that when a hyperpolarized noble gas (*e.g.*, ^{129}Xe) is dissolved in liquid solvents, a time dependent departure of, *e.g.*, the proton spin polarization from its thermal equilibrium is observed. The variation of the magnetization, positive or negative depending on the sign of the spin polarization of the noble gas, is an unexpected manifestation of the nuclear Overhauser effect (NOE), a consequence of cross relaxation between the spins of the solution protons and the dissolved hyperpolarized noble gas. Time-resolved magnetic resonance images of both nuclei, ^1H and dissolved noble gas, in solution show that the proton magnetization is selectively perturbed in regions containing the spin-polarized noble gas. Thus, it has now been determined that optical pumping and the nuclear Overhauser effect can effectively be used to transfer enhanced polarization from hyperpolarized noble gas to solution phase species without requiring the need for radiofrequency irradiation of the perturbing spins, an effect which is denoted Spin Polarization Induced Nuclear Overhauser Effect (SPINOE). Thus, SPINOE can advantageously be used to enhance the sensitivity of NMR and, in turn, to better determine the primary structure, conformation and local dynamic properties of the molecules in a liquid solution.

As such, in one aspect, the present invention provides a method for analyzing a sample containing an NMR active nucleus. This method comprises:

- (a) contacting the sample with a hyperpolarized noble gas; (b) scanning the sample using nuclear magnetic resonance spectroscopy, magnetic resonance imaging, or both nuclear magnetic resonance spectroscopy and magnetic resonance imaging; and (c) detecting the NMR active nucleus, wherein the NMR active nucleus is a nucleus other than a noble gas.

The term "contacting" is used herein interchangeably with the following: combined with, added to, dissolved in, mixed with, passed over, flowed over, administered to, injected into, ingested by, etc. The sample can be contacted with the hyperpolarized noble gas in a liquid, solid or gas phase. Further, the sample studied may 10 be a liquid, solid, a combination of a liquid and a solid or the boundary between a solid and a liquid. Prior to contacting the sample with the hyperpolarized noble gas, it may be desirable to freeze the noble gas to preserve the hyperpolarization. Further, freezing the gas in a magnetic field can preserve the hyperpolarization for a period which is significantly longer than that obtained simply by freezing the gas. For those noble gases 15 which freeze at temperatures which are difficult to achieve, it is within the scope of this invention to cool those gases to a temperature above their freezing point. This procedure is encompassed by the term "freezing." Similar to that described above, such cooling can also occur in the presence of a magnetic field

Once contacted with the noble gas, the sample can be scanned using NMR, 20 MRI or both. The sample is scanned to detect the effects of the hyperpolarized gas on NMR active nuclei within the sample. Any non-noble gas NMR active nucleus can be detected. As used herein, "NMR active nucleus" denotes those nuclei which have a nonzero spin quantum number. Such NMR active nuclei include, but are not limited to, ¹H, ¹³C, ¹⁵N, ¹⁹F, ²⁹Si, ³¹P and combinations thereof. In preferred embodiments, multiple 25 NMR active nuclei are detected. By detecting the effects of the hyperpolarized noble gas on the sample, one can readily analyze the structure, chemistry, spatial distribution, etc. of the sample.

In another aspect, the present invention provides a method for analyzing a sample which is based on the discovery that a noble gas can be combined with a fluid to 30 form a mixture and, in turn, the mixture can be delivered to blood or other tissue while the noble gas still has a large off-equilibrium nuclear spin polarization. Thus, this method comprises: (a) combining a hyperpolarized noble gas with a fluid to form a mixture; (b) contacting the sample with the mixture; and (c) scanning the sample, the noble gas or both the sample and the noble gas by nuclear magnetic resonance spectroscopy, 35 magnetic resonance imaging or both nuclear magnetic resonance spectroscopy and magnetic resonance imaging.

As used herein, the term "fluid" includes, but is not limited to water, saline, phosphate buffered saline, aqueous buffer solutions, fluorocarbons, fluorocarbon

solutions in water or organic solvents, aqueous fluorocarbon emulsions, lipids, solutions of lipids organic solvents, aqueous emulsions of lipids, organic solvents (e.g., DMSO, ethanol, *etc.*). "Aqueous" encompasses solutions and emulsions prepared with $^1\text{H}_2\text{O}$, $^2\text{H}_2\text{O}$ or $^3\text{H}_2\text{O}$. The terms "fluid," "liquid" and "liquid carrier" are used interchangeably herein.

In preferred embodiments, the noble gas is selected from the group consisting of xenon, helium, neon, krypton and mixtures of these gases. In more preferred embodiments, the noble gas is xenon and in particularly preferred embodiments, the noble gas is either ^{129}Xe or ^{131}Xe . In this method, it is desirable to pre-dissolve the hyperpolarized noble gas in a fluid which can, for example, prolong its relaxation time when the hyperpolarized xenon is in contact with physiological fluids. For instance, if the hyperpolarized gas is to be injected into blood, it is desirable to first pre-dissolve the hyperpolarized gas in a lipid, lipid solution or lipid emulsion to form a mixture which, in turn, is injected into the blood. Also desirable is dissolving the hyperpolarized noble gas in a fluorocarbon, fluorocarbon solution or fluorocarbon emulsion. The means of making such lipid and fluorocarbon formulations will be apparent to those of skill in the art. Moreover, it may be desirable to use a hyperpolarized noble gas to polarize a fluid which, in turn, is used as the contrasting agent or probe. For instance, it may be desirable to polarize water by combining it with a hyperpolarized noble gas and, thereafter, use the polarized water as the contrasting agent or probe. It may also prove advantageous to dissolve the noble gas in a liquid prior to hyperpolarizing the noble gas.

In another aspect, the present invention provides a pharmaceutical composition comprising a hyperpolarized noble gas dissolved in a physiologically compatible liquid carrier. In preferred embodiments, the liquid carrier is compatible with administration of the hyperpolarized gas by percutaneous, intravenous, oral, intraperitoneal, intramuscular or inhalation routes. In certain more preferred embodiments, the liquid carrier is appropriate for administration to an organism via an intravenous route.

As noted above, the hyperpolarized noble gas is combined with a fluid or liquid carrier which is chemically, biologically or materially compatible with the sample to be analyzed or, in some instance, dissolves as much of the noble gas as possible. Fluids suitable for use in the methods of the present invention include, but are not limited to, water, saline water, isotonic buffers, lipids, lipid emulsions, organic solvents, fluorocarbon blood substitutes and other medically safe intravenous or oral media in which the noble gas relaxation time is sufficiently long.

In preferred embodiments, the fluid in which the noble gas is dissolved is a fluorocarbon or aqueous perfluorocarbon emulsion. Preferred species are perfluorocarbons including, but not limited to, perfluorodecalin, perfluoro-1,3-dimethylcyclohexane, perfluorohexane(s), perfluorohexyl iodide,

perfluoro(methylcyclohexane), perfluoro(methyldecalin), perfluoro-2-methyl-2-pentene, perfluorononane, perfluorooctane(s), perfluorobutylamine and perfluorotriethylamine. The only caveat to the use of perfluorocarbons is that, where it is desired to use fluorocarbons *in vivo*, the fluorocarbons must be compatible with the biological system under study.

5 Those of skill in the art will readily be able to discern whether the fluorocarbon is compatible with the biological system. For *in vitro* applications, such compatibility is desirable but is not essential.

Particularly preferred fluorocarbons are those known in the art to be safe for *in vivo* administration. Of those safe for *in vivo* administration, perfluorocarbons which are useful as blood substitutes are the most preferred. Perfluorocarbons useful as blood substitutes are known in the art. (See, for example, Long, D.M., *et al.* in BLOOD SUBSTITUTES, Chang, T.M.S. and Geyer, R.D., Eds. Marcel Dekker, Inc. New York, 1989, pp 411-420, which is herein incorporated by reference.). Examples of perfluorocarbons used as blood substitutes include perfluorooctylbromide (PFOB), perfluorotributylamine and perfluorodecalin. Fluorocarbons can be used as neat liquids, emulsions, or they can be dissolved in a solvent or injection adjuvant prior to their use.

Fluorocarbon emulsions can be formed with water, plasma, blood, buffers or other aqueous constituents. Methods of producing pharmaceutically acceptable solutions and emulsions are well known to those of skill in the art and any means known in the art for preparing these mixtures can be used to practice the instant invention. (See, Nairn, J.G., in REMINGTON'S PHARMACEUTICAL SCIENCES, Vol. 17, Gennaro, A.R., Ed., Mack Publishing Co., Easton, PA, 1985, pp. 1492-1517, which is incorporated herein by reference.).

Fluids particularly preferred in practicing the present invention are commercially available blood substitutes such as PFB-1, PFB-2 (Alliance Pharmaceutical Corp.) and FLUOSOL®. FLUOSOL®, an intravascular perfluorocarbon emulsion which is commercially available from Alpha Therapeutic Corporation (Los Angeles, California, U.S.A), is exemplary of a fluorocarbon blood substitute which can be used in the methods of the present invention. Other fluorocarbons and fluorocarbon formulations useful in practicing the invention will be apparent to those of skill in the art.

In another embodiment, the noble gas is dissolved in a lipid, lipid solution or lipid emulsion. The term "lipid" refers to any oil or fatty acid derivative. The oil may be derived from vegetable, mineral or animal sources. As used herein, the term "lipid" also includes those lipids which are capable of forming a bilayer in aqueous medium, such that a hydrophobic portion of the lipid material orients toward the bilayer while a hydrophilic portion orients toward the aqueous phase. Hydrophilic characteristics derive from the presence of phosphato, carboxylic, sulfato, amino, sulphydryl, nitro and other like groups. Hydrophobicity can be conferred by the inclusion of groups that include, but

are not limited to, long chain saturated and unsaturated aliphatic hydrocarbon groups and such groups substituted by one or more aromatic, cycloaliphatic or heterocyclic group(s). Preferred lipids are phosphoglycerides and sphingolipids, representative examples of which include phosphatidylcholine, phosphatidylethanolamine, phosphatidylserine, 5 phosphatidylinositol, phosphatidic acid, palmitoyloleoyl phosphatidylcholine, lysophosphatidylcholine, lysophosphatidyl-ethanolamine, dipalmitoylphosphatidylcholine, dioleoylphosphatidylcholine, distearoyl-phosphatidylcholine or dilinoleoylphosphatidylcholine could be used. Other compounds lacking in phosphorus, such as sphingolipid and glycosphingolipid families, are also within the group designated 10 as lipid. Additionally, the amphipathic lipids described above may be mixed with other lipids including triglycerides and sterols.

Particularly preferred in practicing this embodiment of the present invention is the use of a commercially available lipid preparation such as 10% or 20% INTRALIPID® (Clintec Nutrition, Deerfield, Illinois, U.S.A.), or 10% or 20% LIPOSYN® II, 15 or 10% or 20% LIPOSYN® III. LIPOSYN® is an intravenous fat emulsion which is commercially available from Abbot Laboratories (Abbot Park, Illinois, U.S.A.), and is exemplary of a lipid emulsion which can be used in the methods of the present invention. Lipid emulsions are particularly useful because they dissolve the noble gases and, in addition, because the noble gases have long relaxation times in such lipids. Other lipids, 20 lipid mixtures and fluids in general which are suitable for use in accordance with the present invention will be apparent to those of skill in the art.

It should be noted that it is often desirable to add a deuterated or partially deuterated solvent to the mixture. Moreover, intramuscular injection adjuvants, such as DMSO, vitamin E, etc., can also be used as carriers of the noble gas. Many of these fluids are readily available from commercial sources. Other compounds which are solvents for noble gases and also have pharmaceutically acceptable or pharmacologically useful properties will be apparent to those of skill in the art.

In certain preferred embodiments, the fluid into which the noble gas is dissolved will have the property of specifically or selectively targeting a specific organ or tissue within an organism. Many methods of achieving such targeting are known in the art. For example, lipid vesicles (liposomes) are known to be rapidly scavenged by the cells of the reticuloendothelial system (RES). Thus, in one embodiment, polarized noble gas is targeted to the RES by its incorporation into a liposome. Certain liposomes ("Stealth liposomes") are known which avoid the cells of the RES and remain primarily intravascular over their period of *in vivo* residence. Thus, in another embodiment, the hyperpolarized noble gas is incorporated into a "Stealth liposome" and is used as an intravascular agent. Other liposomes for use in the present invention include temperature-sensitive liposomes, target-sensitive liposomes and pH-sensitive liposomes. Each of these

EXAMPLES

Materials and Methods

The following general materials and methods were used in the examples
described below.

The design of the shaker used in the dissolution stage for xenon mixing and delivery is illustrated in FIG. 1. The shaker has a small sidearm which can be isolated from the main volume by a stopcock. The shaker is charged with a sample of either normal abundance or isotopically enriched xenon (80% ^{129}Xe , EG&G Mound, Miamisburg, Ohio, U.S.A.). Laser polarization is performed prior to admitting the xenon to the shaker. Briefly, approximately 5×10^4 mol of 80% isotopically enriched ^{129}Xe was optically pumped in a 30 cc cylindrical glass pumping cell (diameter \approx 30 mm). Before optical pumping, the cell was cleaned and coated with SURFASIL® (Pierce Chemical Co., Florence, Massachusetts, U.S.A.); the cell was then evacuated to 10^{-6} torr and loaded with one drop of melted rubidium metal in a dry nitrogen environment. Optical pumping was performed with a 1.3 W continuous-wave Ti:sapphire laser (794.7 nm) for 20-30 min, and the temperature of the cell was maintained at 60-80 °C by a temperature-controlled nitrogen gas stream. Typically, the apparatus produces xenon polarization levels in the range of 5-10%.

Following laser polarization, the polarized ^{129}Xe is frozen at liquid nitrogen temperatures in the sidearm in a magnetic field of approximately 50 mT provided by a small permanent magnet. The magnetic field is used in the freezing stage to prevent the decay of xenon polarization. The xenon is sublimated and then admitted into the solution. The small size of the shaker allows for the accumulation of several atmospheres of xenon pressure which aids in increasing the xenon concentration in the solution. During the dissolution procedure, the vessel is vigorously shaken to help dissolve the xenon gas. The resulting xenon solution is extracted with a syringe through a high-pressure rubber septum. In those examples below wherein a solution NMR study is performed on an *in vitro* sample, the xenon is immediately injected into an NMR tube which contains the sample to be studied. The loss of polarization during the injection procedure was found to be insignificant.

EXAMPLE 1

This example describes the ^{129}Xe NMR of a sample of hyperpolarized ^{129}Xe dissolved in aqueous saline. The T_1 of xenon was measured in both H_2O saline and D_2O /saline.

In an NMR tube open to the atmosphere were combined saline and hyperpolarized ^{129}Xe . The saline used had a NaCl concentration of 0.9% by weight.

¹²⁹Xe was dissolved in saline as described in the materials and methods section above. Xenon has a low solubility in saline, with an Ostwald coefficient of only 0.0926 (the standard temperature and pressure volume of xenon dissolved in 1 liter of liquid at 1 atmosphere of gas pressure; 1 atm = 101.3 kPa). In H₂O/saline, the T₁ of xenon is quite long (66 s at 9.4 T). The ¹²⁹Xe NMR spectrum of a solution of ¹²⁹Xe in D₂O saline is displayed in FIG. 2. In saline made with D₂O, the T₁ of xenon is ≈ 1000 s. Thus, the shorter T₁ of xenon in H₂O saline is due to dipolar couplings between the hyperpolarized xenon electrons and the proton nuclear spins.

Example 1 demonstrated the acquisition and characteristics of ¹²⁹Xe spectra of hyperpolarized xenon dissolved in aqueous solution.

EXAMPLE 2

This example demonstrates the use of xenon NMR to study the partition of xenon between the intracellular and extracellular compartments in a sample of human blood. The NMR of xenon in human blood was measured using both hyperpolarized and unpolarized xenon.

2.1 Materials and Methods

A sample of human blood was prepared by allowing fresh blood from a volunteer to settle for a few hours and subsequently decanting off a portion of the plasma. The portion removed accounted for approximately 30% of the total volume of the blood sample. Following removal of a portion of the plasma, xenon saturated saline (1 mL) was injected into the red blood cell (RBC) sample (1 mL) and the ¹²⁹Xe NMR was measured. The NMR spectra were measured on a Bruker AM-400 spectrometer.

2.2 Results

The NMR spectrum of non-polarized xenon was measured in an RBC sample (FIG. 3A). Considerable signal averaging was required in order to obtain a spectrum with an acceptable signal-to-noise ratio. The spectrum was acquired over 1.5 h and is the product of 520 scans. In marked contrast, a spectrum with an excellent signal-to-noise ratio was obtained following one scan when laser-polarized ¹²⁹Xe was used (FIG. 3B). The signal enhancement obtained through using laser-polarized ¹²⁹Xe, rather than non-polarized ¹²⁹Xe, was estimated to be approximately 3 orders of magnitude.

The NMR spectra of both the laser-polarized and non-polarized ¹²⁹Xe in the RBC sample display two peaks; 216 ppm and 192 ppm. The peak at 216 ppm arises from ¹²⁹Xe which has diffused into the RBC. The peak at 192 ppm arises from the ¹²⁹Xe which remains extracellular and is in the saline/plasma mixture. The significant difference between the xenon chemical shift in the RBC and that in the saline/plasma is primarily due to the xenon binding to hemoglobin.

Thus, through the use of laser polarized xenon it is possible to rapidly distinguish between intracellular and extracellular populations of ^{129}Xe . Further, the significantly improved signal-to-noise ratio obtained in spectra measured on samples containing laser polarized ^{129}Xe NMR spectra allows the real time observation of the dynamics of the transfer of the xenon from the saline/plasma mixture into the RBC.

EXAMPLE 3

Example 3 illustrates the use of NMR spectroscopy to observe the dynamics of the mixing of laser polarized ^{129}Xe between the intracellular and extracellular compartments of a sample consisting of red blood cells and plasma.

3.1 Materials and Methods

A sample of laser polarized xenon in saline and a RBC sample were prepared as described in Examples 1 and 2, respectively. By using short rf pulses of small tipping angle, ^{129}Xe NMR spectra were acquired as a function of time after injection of the xenon/saline mixture into the blood. NMR spectra were measured on a Bruker AM-400 spectrometer.

3.2 Results

The results of this experiment are illustrated in FIG. 4. In FIG. 4, the main figure shows the time dependence of the xenon signal in the RBC and in the saline/plasma, normalized by the total signal. The initial rise of the RBC signal and decrease in the saline/plasma signal indicates the transfer of xenon from the saline/plasma water mixture to the RBC during the mixing. Within the first second, the rise in the RBC signal and the reduction of the saline/plasma signal describe the dynamic process of xenon entering the RBC from the saline/plasma during mixing. The time dependence of both the RBC and saline/plasma signals during the mixing process can be described by an exponential function of the form:

$$f(t) = A + B(\exp(-\frac{t}{T})) \quad (2)$$

where A and B are constants and the time constant (T) for this function was estimated to be about 200 ms.

The signal increase (about 1 sec) is probably due to xenon rich blood dripping from the walls of the sample tube into the detection coil after vigorous mixing. The xenon transfer from the water to the red blood cells is evident. The timescale for the process is 170 ± 30 ms. When 1 cc of saline water is mixed with 1 cc of red blood cells, the equilibrium distribution of the integral of the two peaks is approximately 50%. Remarkably, the two peaks decay with the same rate constant (about 5 seconds). Spin-lattice relaxation time of xenon in blood measured with conventional NMR yielded two

different decay rates for the 2 peaks. This is probably an artifact associated with the settling of the red blood cells during the 12 or more hours of data acquisition required for the conventional experiments. After separation of the erythrocytes from the plasma, the xenon exchange between the two compartments is very inefficient, and two different relaxation times are observed. When the red blood cells and the plasma are mixed, the exchange is fast enough to yield the same T_1 for the two peaks. The value for the exchange rate we have measured is consistent with this model. As the experiments have been performed in a sample tube open to air, an additional contribution to the decay of the signal may be due to xenon transfer to the air. Such mechanism would not play a role when the solution is administered intravascularly to tissues.

The inset in FIG. 4 displays the time dependence of the integrated xenon signal from both peaks in the spectra. From the decay starting after 2 seconds, the T_1 of the two components was found to be approximately 5.0 seconds. The initial rise in the total xenon signal intensity during the first second, following the vigorous injection and mixing of the xenon/saline solution, was most likely caused by xenon-containing blood/plasma/saline mixture descending from the walls of the sample tube into the region of the detection coil. Because the sample was unlikely to be intimately mixed and equilibrated at the start of the NMR measurements, the data acquired in the above-described example reflect primarily the xenon mixing process between the RBC and the saline/plasma.

This example illustrates the feasibility of using the techniques of the present invention to study the dynamics of noble gas exchange between the intracellular and extracellular compartments of a tissue.

25

EXAMPLE 4

Example 4 describes the determination, using NMR spectroscopy, of the intrinsic xenon exchange rate between the RBC and the saline/plasma.

4.1 Materials and Methods

A sample of laser polarized xenon in saline and a RBC sample were prepared as described in Examples 1 and 2, respectively. By using short rf pulses of small tipping angle, ^{129}Xe NMR spectra were acquired as a function of time after injection of the xenon/saline mixture into the blood. NMR spectra were measured on a CMX Infinity spectrometer (Chemamagnetics-Otsuka Electronics, Fort Collins, CO, U.S.A.) at a magnetic field of 4.3 Tesla.

35

4.2 Results

The xenon exchange rate between the extracellular and intracellular compartments of a RBC/saline/plasma sample was measured by selectively inverting the xenon saline/plasma NMR line and observing the recovery of the two signals. The

selective inversion was achieved by an amplitude-modulated Gaussian pulse of 1 ms duration centered at the frequency of the saline/plasma signal. This pulse also reduced the absolute signal intensities for the RBC and saline/plasma peaks by about 50%. A field gradient pulse of 1 ms was applied after the inversion pulse to dephase any components of the transverse magnetization. After the inversion pulse, xenon spectra were taken at fixed time intervals using a small tipping angle (20°). Following the addition of the xenon/saline solution into the RBC sample, a delay of 3 seconds before the application of the inversion pulse insured that the xenon/RBC system was well mixed and equilibrated. The results of the experiment are displayed graphically in FIG. 5A and FIG. 5B.

FIG. 5A shows the initial equilibrium spectrum 13 ms before the application of the inversion pulse and three of a series of spectra which were measured after the selective inversion pulse. The exchange of xenon from the RBC to the saline/plasma is shown by the increase in amplitude of the saline/plasma signal and the corresponding reduction in the amplitude of the RBC signal. The time dependence of the signals, S_{RBC} and S_{pl} , can be described by the following equations:

$$S_{RBC} = (S_{RBC}^o + S_{pl}^o) \frac{\tau_{RBC}}{\tau_{RBC} + \tau_{pl}} + S_o \exp(-\frac{t}{\tau}), \quad (3)$$

$$S_{pl} = (S_{RBC}^o + S_{pl}^o) \frac{\tau_{pl}}{\tau_{RBC} + \tau_{pl}} - S_o \exp(-\frac{t}{\tau}), \quad (4)$$

$$S_o = S_{RBC}^o \frac{\tau_{pl}}{\tau_{RBC} + \tau_{pl}} - S_{pl}^o \frac{\tau_{RBC}}{\tau_{RBC} + \tau_{pl}}, \quad (5)$$

where τ_{RBC} and τ_{pl} are residence time constants for xenon in the RBC and saline/plasma, and $1/\tau = 1/\tau_{RBC} + 1/\tau_{pl}$. S_{RBC}^o and S_{pl}^o are the initial intensities for the RBC and the plasma/saline components, respectively, immediately after the inversion pulse. The effect of the spin-lattice relaxation is neglected since $\tau < < T_1$, making $S_{RBC}^o + S_{pl}^o$ a constant during the exchange process.

The time dependence of the difference of the two signals, $\Delta S = S_{RBC}^o - S_{pl}^o$, is shown in FIG. 5B. From an exponential fit, it was determined that $\tau = 12.0 \pm 1$ ms. The reduction of the signals due to the finite tipping angle was taken into account. Given the constraint on τ_{pl}/τ_{RBC} from the ratio of the signals at equilibrium, $\tau_{RBC} = 20.4 \pm 2$ ms, $\tau_{pl} = 29.1 \pm 2$ ms were obtained. The time scale for the diffusion of xenon ($\tau_{RBC} = 20.4$ ms) corresponded to the time for the diffusion of xenon over a distance of 11 μm (a diffusion constant of $10^{-5}\text{ cm}^2/\text{s}$ was assumed). This distance is slightly larger

than the characteristic dimension of the RBC. The xenon τ_{RBC} was found to be longer than that for water molecules, which was determined to be 12 ± 2 ms at room temperature, Herbst, M.D., *et al.*, *Am. J. Physiol.*, 256: C1097-C1104 (1989).

5 The above example demonstrates that data relevant to the dynamics of the interaction between laser polarized xenon and its environment (e.g., a mixture of red blood cells and plasma) are accessible using NMR spectroscopy.

EXAMPLE 5

This example illustrates the preparation and NMR properties of a vehicle
10 for xenon delivery which consists of a mixture of xenon and an aqueous suspension of lipid vesicles. An efficient method is provided for delivery of optically polarized xenon to the vascular system in order to observe the xenon-129 NMR signal before the xenon polarization has decayed. Specifically, the hyperpolarized gas is pre-dissolved in
15 solutions where the xenon has a long spin-lattice relaxation time and, thereafter, the xenon/solution mixture is administered to the blood.

5.1 Materials and Methods

A solution of hyperpolarized xenon in INTRALIPID® was prepared in the same manner as described for the saline solution of hyperpolarized xenon, however, the shaker was charged with INTRALIPID® rather than saline. INTRALIPID® solutions consist
20 of aqueous suspensions of lipid vesicles of approximately $0.1\mu\text{m}$ in diameter, which are well tolerated *in vivo* and are used clinically as nutrient supplements. Commercially available 20% INTRALIPID® solution (Pharmacia, Uppsala, Sweden) is approved by the U.S. Food and Drug Administration for use in humans. Importantly, xenon has an approximately 4-fold greater solubility in INTRALIPID® than in saline. The INTRALIPID®
25 solution was charged with laser polarized ^{129}Xe and an aliquot (1 mL) of this solution was added to human blood (1 mL). The spectra were obtained on a Bruker AM-400 spectrometer. The 128×64 image was obtained by the Echo Planar Imaging method on a Quest 4300 (Nalorac Cryogenics, Martinez, CA, U.S.A.) spectrometer.

5.2 Results

30 The xenon T_1 in the INTRALIPID® solution was measured to be 40 ± 3 s. The spectrum of the laser polarized xenon, delivered to blood as an Intralipid solution, is shown in FIG. 6A. The predominant feature of the spectrum is a peak at 194 ppm, which corresponds to the xenon in the pure Intralipid solution. Only a small signal is observed at 216 ppm; the signal corresponding to xenon in the RBC (*i.e.*, intracellular).
35 The ratio of the peak corresponding to xenon in the INTRALIPID® solution and the peak from the intracellular xenon is approximately 6:1. This result is consistent with a higher affinity of the xenon for the lipids and a correspondingly inefficient transfer into the RBC. The T_1 decay time of the signal at 194 ppm was measured to be 16 s, a factor

approximately 3-fold larger than the corresponding decay time for xenon in the saline water/blood mixture. The ^{129}Xe signal was so strong in this sample as to allow the direct imaging of the xenon distribution in the mixture. The acquired image is displayed in FIG. 6A (inset).

5 Xenon in blood can be utilized to study lung air-space anatomy, tissue perfusion and NMR angiography. In general, hyperpolarized xenon NMR would be an alternative to the imaging techniques that make use of radioactive isotopes of xenon, such as ^{127}Xe and ^{133}Xe . The advantages of MRI of hyperpolarized xenon are the zero ionizing radiation dose absorption by the patient and a potentially much better spatial
10 resolution. NMR of xenon may also prove useful for brain studies. Specifically, magnetic resonance imaging of hyperpolarized xenon would enable better detection of central nervous system perfusion and thus be a tool for diagnosis of stroke and also a flow specific tool for functional imaging.

15 This example demonstrates the preparation and the properties of solutions of hyperpolarized xenon in lipids. Also demonstrated is the principle that lipid solutions of laser polarized xenon can be used to deliver polarized xenon through the blood. The presence of the lipid in the delivery vehicle both retards penetration of the xenon through the RBC membrane and protects the xenon polarization from rapidly decaying.

20 The use of different solutions for administering hyperpolarized xenon to blood and tissues is very promising for ^{129}Xe Spectroscopic Imaging, Chemical Shift Imaging or *in vivo* Localized NMR Spectroscopy in tissues. ^{129}Xe NMR parameters, such as the relaxation times, may prove useful to probe the state of health of tissues or the malignancy of tumors. Moreover, xenon dissolves readily in fat, and hyperpolarized xenon MRI may be an alternative to conventional proton MRI of fatty tissues.
25

EXAMPLE 6

Example 6 demonstrates the utility of perfluorocarbons as delivery vehicles for laser polarized xenon.

30 Perfluorocarbon compounds are generally chemically inert and non-toxic. Interestingly, perfluorocarbon emulsions are able to absorb and transport oxygen and carbon dioxide. A representative perfluorocarbon emulsion, FLUOSOL® (Green Cross, Osaka, Japan), was chosen as a promising prototypical delivery vehicle for xenon. FLUOSOL® is an emulsion which contains 20% perfluorocarbon and is approved by the U.S. F.D.A. for intravascular administration in humans as a blood substitute.

35 A solution of hyperpolarized xenon in FLUOSOL® was prepared in the same manner as described for the saline solution of hyperpolarized xenon, however, the shaker was charged with FLUOSOL® rather than saline. The FLUOSOL® solution was charged

with laser polarized ^{129}Xe and an aliquot (1 mL) of this solution was added to human blood (1 mL). The spectra were obtained on a Bruker AM-400 spectrometer.

6.2 Results

FIG. 6B shows a ^{129}Xe NMR spectrum acquired after mixing the FLUOSOL®/xenon solution with blood. The peak at 216 ppm corresponds to xenon in the RBC, whereas the broad peak centered around 110 ppm (FIG. 6B, inset) arises from xenon in the FLUOSOL® solution. Xenon in pure FLUOSOL® has a chemical shift of 110 ppm and the peak exhibits a broadening which is similar to that observed in the spectrum of the xenon/blood/FLUOSOL® solution. The ratio of the integrated intensities of the broad and narrow peaks is approximately 3. The T_1 of the narrow peak was measured to be 13 ± 1 s. This T_1 is, similar to that measured for xenon in INTRALIPID®, longer than that measured for xenon in the RBC/plasma sample. The results with FLUOSOL® suggest that xenon exchanges between the interior of the RBC and an environment characterized by a xenon relaxation time which is longer than that exhibited by intracellular xenon. Presumably, the xenon which has the longer relaxation time resides in the FLUOSOL®. These results have implications for the selective MRI/NMR of xenon which has been transferred to tissues.

Also acquired was a two-dimensional MR image of ^{129}Xe dissolved in fresh human blood (FIG. 7). The image was acquired immediately after the blood was mixed with a saline solution saturated with hyperpolarized ^{129}Xe .

The above example illustrates that perfluorocarbon emulsions are useful delivery vehicles for hyperpolarized noble gases. Also demonstrated is the feasibility of acquiring an MR image of ^{129}Xe dissolved in blood when the ^{129}Xe is administered to the blood as a saline solution and, therefore, has a shorter T_1 than is observed for ^{129}Xe in a fluorocarbon delivery agent.

EXAMPLE 7

7.1 Materials and Methods

Solutions of hyperpolarized ^{129}Xe in partially deuterated benzene (25% $\text{C}_6\text{D}_5\text{H}$, 75% C_6D_6) were prepared as described above for saline solutions of ^{129}Xe with the exception that the shaker was charged with the benzene solution rather than saline. Typically, 4×10^4 mol of enriched ^{129}Xe (80%, EG&G Mound) were used in one experiment at a pressure of 1 atm. ^{129}Xe NMR was performed at 51 MHz on a Quest 4300 spectrometer (Nalorac Cryogenics, Martinez, California, U.S.A.) with a home built probe and a tipping angle of 3° . ^1H NMR was performed at 185 MHz with a home built probe and a tipping angle of 3° .

Time-resolved two-dimensional MR images of ^{129}Xe were obtained using the fast low-angle shot (FLASH) imaging method on the Quest 4300 instrument using a

tipping angle of 3° for each of the 64 signal acquisitions. The frequency-encoding gradient was 3.5 G/mm. The step size of the phase-encoding gradient pulses, which were 500 μ s long, was 0.063 G/mm. The diameter of the sample tube was 7 mm and the solution occupied a region within the tube of length 15 mm. The images were 64 x 5 128 pixel images.

The time-resolved distribution (in seconds) of an unshaken sample of partially deuterated benzene was obtained from MRI projections along the tube axis (z). The imaging field gradient for the acquisition of these images was 2.6 G/mm.

Two-dimensional MR images of the SPINOE-enhanced ^1H signals were obtained at 2 and 6 minutes after hyperpolarized ^{129}Xe was admitted to the sample tube containing normal benzene. The images were taken by the echo planar imaging method in 24 ms. The frequency encoding gradient was 3.15 G/mm; the phase-encoding gradient pulses were 0.14 G/mm and 50 μ s long. The image dimension was 128 x 32 pixels, and the image was zero-filled to 256 x 256 pixels in data processing.

The methods used and the results obtained in this example are discussed in detail in Navon, G., *et al.*, *Science*, 271: 1848-1851 (1996), which is herein incorporated by reference.

7.2 Results

In the following example, the preliminary experiments designed to probe the SPINOE between hyperpolarized xenon and protons in solution are described. When hyperpolarized ^{129}Xe is dissolved in liquids, a time-dependent departure of the proton spin from its thermal equilibrium was observed. The variation in magnetization was an unexpected manifestation of the nuclear Overhauser effect (NOE), a consequence of cross-relaxation between the spins of solution protons and ^{129}Xe . SPINOE has been used to monitor time dependent magnetic resonance images and high resolution NMR spectra of solution spins as they encounter the migrating xenon atoms.

The time dependence of the ^{129}Xe NMR signal intensity observed when hyperpolarized ^{129}Xe is dissolved in liquid benzene is shown in FIG. 8. The observed spin-lattice relaxation time of ^{129}Xe in solution, a combination of the gas and solution relaxation times, is ~200s in normal benzene and ~1000s in the partially deuterated sample (Moschos, A., *et al.*, *J. Magn. Reson.* 95: 603 (1991); and Diehl, P., *et al.*, *J. Magn. Reson.* 88: 660 (1990)). The difference between these two values demonstrates the effect of magnetic dipolar coupling between ^1H and ^{129}Xe spins on the relaxation of the ^{129}Xe magnetization; the same coupling underlies the cross relaxation between the xenon and proton spin systems. For the initial NOE experiments, the partially deuterated liquids were used to promote the effects of cross relaxation over the potentially limiting auto-relaxation of the proton spins.

The effect of the dissolved hyperpolarized ^{129}Xe on the ^1H magnetization in liquid benzene is illustrated in FIG. 9. The proton NMR signal exhibits a positive or negative time-dependent NOE, depending on the sign of the ^{129}Xe magnetization, which is determined by the helicity of the laser light or the orientation of the magnetic field in the optical pumping stage. The fractional enhancement of the proton magnetization over its thermal equilibrium value is typically ~ 0.1 for benzene, and between 0.5 and 2 for the partially deuterated sample.

Based on the theory of the nuclear Overhauser effect, the following expression can be derived for the maximum change in the polarization of the solvent nuclei (I) due to cross relaxation with the dissolved gas (S) :

$$\frac{I_z(t_0) - I_0}{I_0} = - \frac{\sigma_{IS}}{\rho_I} \frac{\gamma_s S(S+1)}{\gamma_I I(I+1)} \frac{[S_z(t_0) - S_0]}{S_0} \quad (6)$$

where γ_s and γ_I are the magnetogyric ratios of the nuclear spins, σ_{IS} the cross-relaxation rate, and ρ_I is the auto-relaxation rate of the I spins. The cross-relaxation rate σ_{IS} has the same value, $\sigma_{IS} = 1.9 \times 10^{-6} \text{s}^{-1}$, for both benzene and partially deuterated benzene solutions, so the difference in the maximum enhancement of the proton polarization in these two solutions originates from the different proton relaxation rates, $\rho_I = (20\text{s})^{-1}$ in benzene and $\rho_I = (160\text{s})^{-1}$ in the partially deuterated solution. Given the spin quantum numbers and the magnetogyric ratios of the two nuclei, $I = S = 1/2$, $\gamma_I = 2.67 \times 10^8 \text{ rad T}^{-1}\text{s}^{-1}$, and $\gamma_s = -7.44 \times 10^7 \text{ rad T}^{-1}\text{s}^{-1}$, and the enhancement of the ^{129}Xe polarization at the time t_0 when the proton magnetization reaches its maximum (minimum), $S_z(t_0)/S_0 \approx 6000$, the maximum proton enhancement is estimated to be 0.06 in C_6H_6 and 0.5 in the partially deuterated solution, in general agreement with the measured values.

The high spin-polarization and the slow relaxation of ^{129}Xe in the solvent allow for a detailed observation of the dissolution process and the flow of xenon in the solvent by means of MRI. FIG. 10 shows two-dimensional MRI projections along the vertical axis of the sample tube. Xenon is found to accumulate first at the bottom of the tube, establishing a gradient in xenon concentration and continues to dissolve into the benzene as the solution gradually becomes saturated. A detail of this process is shown in FIG. 11, where a series of the one-dimensional image intensities along the tube axis reflects the time-dependent spatial distribution of the xenon. The descent of xenon in the sample tube occurs because of density differences between the solution and pure benzene. The heavier xenon-rich regions of the solution, which form at the top of the solution by diffusion of the xenon into the solvent, gravitate to the lower part of the tube by natural convection, ultimately filling the tube with saturated xenon solution.

Because of the SPINOE enhancement of the proton spins proximate to the dissolved hyperpolarized xenon, the xenon concentration gradient is expected to induce a gradient in the proton magnetization. Indeed, as shown in FIG. 12, the benzene proton magnetization images display a time dependent gradient consistent with the spatial distribution of xenon shown in FIGS. 10 and 11. In fact, differential SPINOE
5 enhancements of proton NMR can be observed in solutions containing more than one component or in molecules possessing nuclei with different chemical shifts, making it possible to explore the partitioning and selective association of the hyperpolarized gas.

The foregoing results indicate that it is possible to image not only the hyperpolarized xenon, but also the environment in which it is accommodated, a finding which has implications for both materials and medical applications, for xenon as well as for helium. Because the equilibrium polarization of the solution spins, S_0 , is proportional to the magnetic field, B_0 , the relative SPINOE is inversely proportional to B_0 and is thus expected to be more pronounced at the lower magnetic fields normally used in medical imaging. Furthermore, since the nuclear Overhauser effect depends on the proximity of the xenon nucleus and the neighboring spins, as well as their relative translational motion, a large SPINOE is anticipated in systems where the noble gas atoms are partially immobilized in materials, Miller, J.B., *et al.*, *Macromolecules* 26: 5602 (1993), or temporarily bound to molecules such as proteins, Tilton, R.F., *et al.*, *Biochemistry* 21, 15 6850 (1982), even in the presence of relatively fast proton relaxation. The window is thus opened to other potential applications where xenon may be adsorbed in materials, on surfaces, or in biological molecules and organisms.
20

EXAMPLE 8

This example illustrates the utility of ^{129}Xe - ^1H SPINOE spectroscopy for studying the dynamical and structural characteristics of molecules in solution. That the coupling between laser-polarized ^{129}Xe and protons in a p-nitrotoluene solution is due to nuclear spin dipolar coupling modulated by diffusive motion is demonstrated.
25

8.1 Materials and Methods

The samples were generally prepared as described in the examples above. The pulse sequence used to obtain SPINOE data is a heteronuclear version of the difference NOE pulse sequence originally suggested by Stonehoud, J., *et. al.* *J. Am. Chem. Soc.* 116: 6037 (1994) for homonuclear NOE studies. One method for observing SPINOEs is simply to acquire the proton signal as a function of time after laser-polarized ^{129}Xe is introduced to the solution. The deviation of the proton signal from its thermal equilibrium value determines the signal due to SPINOE from laser-polarized ^{129}Xe . However, this method relies on a subtraction of two large signals (with and without SPINOE), and this subtraction limits the sensitivity of the experiment to only
30
35

those SPINOE signals greater than about one percent of the equilibrium signal. This new sequence is advantageous compared to the conventional SPINOE method since the equilibrium signal can be suppressed by two orders of magnitude or more. This type of sequence has enabled measurements of NOEs less than 10^{-4} of the equilibrium signal.

The difference SPINOE sequence is shown in Fig. 13. The saturation of proton resonances is first achieved by applying a train of proton $\pi/2$ pulses, and this saturation is maintained with the proton π pulses during the mixing time when the SPINOE occurs. The timing of the π pulses is adjusted to give optimal saturation. A π pulse is also applied to the ^{129}Xe resonance at the same time of the proton π pulse so that the proton signal due to SPINOE will be accumulated over the entire mixing time. Odd numbers of such π pulse pairs were used so that each acquisition inverted the ^{129}Xe magnetization; thus the subtraction of two consecutive signals effectively removed all contributions to the signal that did not originate from SPINOE.

8.2 Results

Polarization transfer from laser-polarized xenon to *p*-nitrotoluene in a solution of perdeuterated benzene was observed. *p*-nitrotoluene is a simple molecule that does not show binding of xenon in solution; thus we anticipated that its couplings of its protons to xenon would be similar to that of benzene protons. The difference SPINOE proton spectra with laser-polarized ^{129}Xe are shown in FIG. 14A and FIG. 14B. The ^{129}Xe polarization is negative in FIG. 14A and positive in FIG. 14B and the magnetization transfer to proton is found to be negative and positive, respectively. This observation is consistent with a correlation time that is much shorter than the inverse of the Larmor frequencies of ^1H and ^{129}Xe , in which case the cross-relaxation constant σ_{IS} would be positive. From the initial rise of the proton SPINOE signal intensity, we obtain the values of σ_{IS} for the aromatic and methyl protons to be similar to that for benzene protons and the theoretical estimate of the cross-relaxation rate due to dipolar coupling modulated by molecular diffusion.

The above example demonstrates the utility of $^{129}\text{Xe} - ^1\text{H}$ SPINOE spectroscopy for studying the dynamical and structural characteristics of molecules in solution. That the coupling between laser-polarized ^{129}Xe and protons in a *p*-nitrotoluene solution is due to nuclear spin dipolar coupling modulated by diffusive motion is demonstrated. Further, it has been shown that the sign of the SPINOE signal is influenced by the sign of the ^{129}Xe polarization.

EXAMPLE 9

This example demonstrates the effect of ^{129}Xe binding to a molecule in solution on the observed SPINOE signal(s) arising from that molecule. A cyclic polysaccharide, cyclodextrin, was chosen as a model compound.

9.1 Materials and Methods

Hyperpolarized xenon and mixtures of hyperpolarized xenon and cyclodextrins were prepared generally as discussed above. SPINOE signals of 0.05 M cyclodextrin solutions in deuterated DMSO were measured as described above in Example 8.

9.2 Results

α -Cyclodextrin is a naturally occurring host molecule composed of six D-glucose units linked head to tail in a 1 α , 4-relationship to form a ring known as a cyclohexaamylose. It has a relatively inflexible doughnut shaped structure where the top of the molecule has twelve hydroxyl groups from positions 2 and 3 of the glucose units and the bottom has the 6 primary hydroxyl groups from position 6. The equilibrium proton spectrum of α -cyclodextrin in deuterated DMSO is displayed in FIG. 15. Cyclodextrins are cyclic glucopyranose oligomers that possess a hydrophobic binding pocket, Saenger, W., *Angew. Chem. Int. Ed.* 19: 344 (1980). The hydrophobic binding properties of cyclodextrins permit them to complex a number of different guest species, from drugs to noble gases, Szejtli, J., CYCLODEXTRIN TECHNOLOGY, Kluwer-Academic, Dordrecht, 1988. Specifically, it has been shown in NMR studies that α -cyclodextrin complexes xenon, Bartik, K., *et al.*, *J. Magn. Res. B*, 109: 164 (1995).

The first evidence of strong couplings between xenon and α -cyclodextrin is the reduced ^{129}Xe T_1 in the solution of α -cyclodextrin. For example, the measured ^{129}Xe T_1 was 20 s in 0.1 M α -cyclodextrin solution in deuterated DMSO, compared to a $T_1 > 500$ s in 0.1 M *p*-nitrotoluene in deuterated benzene. This increase in the apparent relaxation rate of xenon is due to the dipolar coupling between xenon and the protons of α -cyclodextrin; this coupling not only determines the cross-relaxation of the two spins, but also contributes to the xenon auto-relaxation.

In order to study the effects of xenon binding on ^{129}Xe - ^1H SPINOE, SPINOEs from laser-polarized xenon to α -cyclodextrin dissolved in a solution of perdeuterated dimethyl sulfoxide (DMSO) were observed. The proton SPINOE spectra of α -cyclodextrin in the presence of ^{129}Xe of negative polarization and of positive polarization are shown in FIG. 16 and FIG. 17, respectively. The assignment of the proton resonance has been reported in other work, Djedaini, F., *et al.*, *J. Mol. Struct.*, 239: 161 (1990). In contrast to the SPINOE spectra of *p*-nitrotoluene, the SPINOE signal intensities for various protons of α -cyclodextrin are substantially different. The strongest SPINOEs are observed from H3 and H5, protons located on the inside of the cyclodextrin cavity. The SPINOE signals from the outer protons H2, H4, and H1, however, are about a factor of 6 smaller. This difference in the xenon coupling to various protons can be expected because such dipolar coupling is highly sensitive to the

relative distance between spins. One can derive a ratio of the distances between xenon-H3,H5 and xenon-H1,H2,H4 to be $1/\sqrt[6]{6} = 1/1.35$.

5 The percentage SPINOE signal is significantly larger than that from *p*-nitrotoluene solution. Taking into account the xenon pressures in the sample cell and the magnetic fields applied in the different experiments of *p*-nitrotoluene and α -cyclodextrin, we estimate that the ratio of the cross-relaxation rates of α -cyclodextrin and *p*-nitrotoluene is approximately 100. This large increase in the overall coupling constant can be attributed to significant binding between xenon and α -cyclodextrin molecules.

10 Although smaller, the SPINOE signals from the three hydroxyl protons are also observable.

15 Additionally, the xenon coupling constants have been compared for α -cyclodextrin and β -cyclodextrin, where β -cyclodextrin is a seven-unit cyclodextrin ring. Even though the size of β -cyclodextrin is merely 15% larger than α -cyclodextrin, its binding of xenon is dramatically reduced and the coupling constants are two orders of magnitude smaller, essentially equivalent to the coupling constants of *p*-nitrotoluene.

20 In the above example, it was demonstrated that the off-equilibrium polarization of xenon can be transferred to other nuclear species, such as protons. Thus, hyperpolarized xenon can be exploited as a contrast agent for protons. Moreover, it can be used to elucidate structures of biologically relevant molecules, such as proteins, by selective polarization transfer to the protons of the specific sites where the xenon binds.

EXAMPLE 10

25 This example describes the *in vivo* use of hyperpolarized xenon dissolved into a lipid vehicle. Optically pumped xenon was dissolved into a lipid emulsion as described in Example 5 and injected intravenously into a rat. The ^{129}Xe NMR spectra from the region of the heart and liver were recorded as a function of time.

10.1 Materials and Methods

30 The laser polarized xenon and the solution of laser polarized xenon in INTRALIPID[®] were prepared essentially as described in the preceding examples.

35 Male rats weighing 200-250 grams were anesthetized by intramuscular injection of ketamine/xylazine/acepromazine (30/3/0.6 mg/kg). Supplemental intramuscular doses were administered as needed to maintain anesthesia. A venous catheter was placed into a tail vein, and the receiver/transmitter surface coil was placed over the heart and liver (FIG. 18). Acquisitions began at start of the injection. Prior to each experiment the rat was placed in lateral recumbency into the magnet. At the conclusion of each experiment, the catheter was removed and the rat was returned to its cage to recover from anesthesia.

The ^{129}Xe NMR spectra were obtained on a home-built NMR spectrometer interfaced with a Bruker 2.35 T magnet (xenon frequency: 27.68 MHz, bore diameter: 25 cm). The receiver-transmitter surface coil had a diameter of 3.5 cm. For the spectroscopy experiment, spectra were obtained every second (pulse angle: $\approx 20^\circ$).
5

10.2 Results

A series of xenon NMR spectra were taken from the beginning of the intravenous injection of the xenon/INTRALIPID® solution. A spectrum representing an average of the sixth through twelfth scans is shown in FIG 19; the time-dependence of 10 the integrated signal is shown in the inset. It was anticipated that the Intralipid would initially accumulate in the liver; it is likely that the initial rise in signal amplitude reflects this accumulation, while the subsequent decay is due to wash-out, xenon relaxation, and the application of rf pulses.

This example demonstrates the feasibility of using lipid solutions of 15 hyperpolarized xenon to deliver the xenon via an intravenous administration route. Also illustrated is that *in vivo* spectra of the hyperpolarized xenon can be readily obtained.

EXAMPLE 11

This example describes the use of ^{129}Xe MR imaging to obtain images of 20 the *in vivo* distribution of hyperpolarized xenon in the rat. The hyperpolarized xenon was administered intramuscularly as a saline solution.

11.1 Materials and Methods

The methods for preparing the hyperpolarized xenon and a saline solution of the hyperpolarized xenon have been described in previous examples. The rats, 25 anesthesia and apparatus were as described in Example 10, above. For the imaging experiment, the catheter was placed in the muscle of the rats thigh and secured with tape. The surface coil was placed over the injection site on the rat's thigh. At the conclusion of the experiment, the catheter was removed and the rat was returned to the cage to recover from anesthesia.

Axial images were acquired perpendicular to the coil using the FLASH 30 sequence shown in FIG. 20. In the imaging experiment, ten two-dimensional ^{129}Xe MR images were taken at intervals of approximately 7 s (with the exception of an 18 s delay between images 5 and 6) from the beginning of the injection of the xenon/saline solution.

11.2 Results

Six of the images obtained are shown in FIG. 21, and depict the signal 35 intensity of the optically pumped xenon in the upper part of the rat's hind leg. The central region of low xenon signal intensity likely corresponds to the rat's femur. From the six images, one may observe that the signal intensity rises quickly and reaches a

maximum at the second image (b) (7 s after the start of the injection), and then decays in the following images. The initial rise in intensity is due to the accumulation of the xenon/saline solution from the injection, while the subsequent decay is due mostly to the application of the rf pulses (48 pulses of approximately 5 degrees tipping angle), although xenon relaxation and wash-out undoubtedly made additional contributions to this decay. The change in the pattern of the images suggests that part of the xenon/saline solution may have penetrated and diffused into the surrounding tissue over the duration of the experiment.

5

The major advantage of saline water as the xenon solvent is the long xenon T_1 , which permits negligible loss of polarization over the injection time. However, the solubility of xenon in saline water is low with an Ostwald coefficient of only 0.0926 (the STP volume of xenon dissolved in 1 liter of liquid at 1 atm of gas pressure). Higher xenon concentrations can be obtained by using alternative xenon solvents (e.g. INTRALIPID® and FLUOSOL®). Furthermore, the xenon partitioning properties of such solvents in biological tissues allow particular *in vivo* applications. It was determined in previous *in vitro* studies that such solvents can bring about a three-fold increase in the effective relaxation time of xenon in blood. Thus, administration of the polarized xenon dissolved into one of these two classes of delivery vehicles is anticipated to improve the MR images acquired and to afford a longer temporal imaging window.

10

15

20

Example 11 demonstrates that *in vivo* ^{129}Xe MR images can be obtained and used to study the distribution of hyperpolarized xenon in a living system.

25

It is to be understood that the above description and examples are intended to be illustrative and not restrictive. Many embodiments will be apparent to those of skill in the art upon reading the above description and examples. The scope of the invention should, therefore, be determined not with reference to the above description and examples, but should instead be determined with reference to the appended claims, along with the full scope of equivalents to which such claims are entitled. The disclosures of all articles and references, including patent applications and publications, are incorporated herein by reference for all purpose.

WHAT IS CLAIMED IS:

1. A method for analyzing a sample containing an NMR active nucleus, said method comprising:
 - (a) contacting said sample with a hyperpolarized noble gas;
 - (b) scanning said sample by nuclear magnetic resonance spectroscopy, magnetic resonance imaging, or both nuclear magnetic resonance spectroscopy and magnetic resonance imaging; and
 - (c) detecting said NMR active nucleus, wherein said NMR active nucleus is a nucleus other than a noble gas.
 2. A method according to claim 1 in which said NMR active nucleus is a member selected from the group consisting of ^1H , ^{13}C , ^{15}N , ^{19}F , ^{29}Si , ^{31}P and combinations thereof.
 3. A method for analyzing a sample, said method comprising:
 - (a) combining a hyperpolarized noble gas with a fluid to form a mixture;
 - (b) contacting said sample with said mixture; and
 - (c) scanning said sample, said noble gas or both said sample and said noble gas by nuclear magnetic resonance spectroscopy, magnetic resonance imaging, or both nuclear magnetic resonance and magnetic resonance imaging.
 4. A method in accordance with claim 3 in which said noble gas is a member selected from the group consisting of xenon, helium, neon, krypton and mixtures thereof.
 5. A method in accordance with claim 3 in which said noble gas is xenon.
 6. A method in accordance with claim 5 in which said xenon is a member selected from the group consisting of ^{129}Xe and ^{131}Xe .
 7. A method in accordance with claim 3 in which said noble gas is ^3He .
 8. The method in accordance with claim 3 further comprising the step of hyperpolarizing said noble gas prior to step (a).

1 9. The method in accordance with claim 8 in which said hyperpolarizing
2 step comprises hyperpolarizing said noble gas through spin exchange with an alkali
3 metal.

1 10. The method in accordance with claim 8 in which said hyperpolarizing
2 step comprises hyperpolarizing said noble gas through metastability exchange.

1 11. The method in accordance with claim 8 in which said hyperpolarizing
2 step comprises irradiating said alkali metal with circularly polarized light.

1 12. The method in accordance with claim 9 in which said alkali metal is
2 selected from the group consisting of ^{23}Na , ^{39}K , ^{133}Ce , ^{85}Rb and ^{87}Rb .

1 13. A method in accordance with claim 3 further comprising freezing said
2 hyperpolarized noble gas to a solid form prior to step (a).

1 14. A method in accordance with claim 3 in which said fluid is a member
2 selected from the group consisting of water, physiological saline, fluorocarbons,
3 fluorocarbon emulsions, lipids, lipid emulsions and blood replacement preparations.

1 15. A method in accordance with claim 3 in which said sample comprises an
2 organism or a portion of an organism.

1 16. A method according to claim 15 in which said portion of an organism
2 comprises an organ or tissue.

1 17. A method in accordance with claim 3 in which said sample is an organic
2 or inorganic monomer.

1 18. A method in accordance with claim 3 in which said sample is an organic
2 or inorganic polymer.

1 19. A method in accordance with claim 3 in which said sample is a
2 biopolymer.

1 20. A method in accordance with claim 19 in which said biopolymer is a
2 member selected from the group consisting of oligopeptides, polypeptides, antibodies and
3 proteins.

1 21. A method in accordance with claim 19 in which said biopolymer is a
2 member selected from the group consisting of oligonucleotides, RNA, mRNA, tRNA,
3 DNA, chromosomes, genes and plasmids.

1 22. A method in accordance with claim 19 in which said biopolymer is a
2 member selected from the group consisting of oligosaccharides, polysaccharides,
3 glycoproteins, and mucopolysaccharides.

1 23. A method in accordance with claim 3 in which said sample is scanned to
2 detect a change in NMR active nuclei caused by said hyperpolarized noble gas.

1 24. A method in accordance with claim 23 in which said NMR active nuclei
2 is a member selected from the group consisting of ^1H , ^{13}C , ^{15}N , ^{19}F , ^{29}Si , ^{31}P and
3 combinations thereof.

1 25. A pharmaceutical composition, comprising a hyperpolarized noble gas
2 dissolved in a physiologically compatible liquid carrier.

1 26. A pharmaceutical composition according to claim 25 in which said liquid
2 carrier is compatible with an administration route which is a member selected from the
3 group consisting of percutaneous, inhalation, intravascular, oral, intraperitoneal and
4 intramuscular.

1 27. A pharmaceutical composition according to claim 25 in which said liquid
2 carrier is a member selected from the group consisting of water, saline, blood, plasma,
3 fluorocarbons, fluorocarbon emulsions, lipids, lipid emulsions, dimethylsulfoxide and
4 vitamin E.

1 28. A pharmaceutical composition according to claim 25 in which said liquid
2 carrier is appropriate for intravenous administration and is a member selected from the
3 group consisting of lipid emulsions and fluorocarbon emulsions.

1 29. A method for producing a pharmaceutical composition according to
2 claim 25, comprising:

- 3 (a) hyperpolarizing a noble gas; and
4 (b) contacting a physiologically compatible liquid carrier with said hyperpolarized
5 noble gas.

1 30. A method according to claim 29 in which step (b) comprises:

- 2 (a) freezing said hyperpolarized noble gas to preserve
3 hyperpolarization; and
4 (b) sublimating said frozen hyperpolarized noble gas into said
5 physiologically compatible liquid carrier, thereby contacting said
6 physiologically compatible liquid carrier with said hyperpolarized
7 noble gas.

1 31. A method for studying a property of a noble gas in a tissue, comprising:

- 2 (a) hyperpolarizing a noble gas;
3 (b) dissolving said hyperpolarized noble gas in a physiologically
4 compatible liquid carrier to form a mixture;
5 (c) contacting said tissue with said mixture from (b); and,
6 (d) scanning said tissue by nuclear magnetic resonance spectroscopy,
7 magnetic resonance imaging, or both, whereby said property is
8 studied.

1 32. A method according to claim 31 in which said property is a member
2 selected from the group consisting of NMR parameters, rate of exchange of said
3 hyperpolarized noble gas between an extracellular compartment and an intracellular
4 compartment of said tissue, concentration of said hyperpolarized gas within said
5 intracellular compartment, concentration of said hyperpolarized gas within said
6 extracellular compartment, relaxation time of said hyperpolarized gas within said
7 intracellular compartment and relaxation time of said hyperpolarized gas within said
8 extracellular compartment.

1 33. A method according to claim 31, wherein said tissue comprises a
2 member selected from the group consisting of blood, muscle, peripheral nervous system
3 tissue and central nervous system tissue.

1 34. A method according to claim 31, wherein said tissue is a central nervous
2 system tissue which is a member selected from the group consisting of brain, spinal cord,
3 cerebrospinal fluid and blood-brain barrier.

1 35. A method for enhancing the relaxation time of a hyperpolarized noble
2 gas in contact with a physiological fluid, comprising:

- 3 (a) forming a hyperpolarized noble gas intermediate solution by dissolving said
4 hyperpolarized noble gas in a fluid in which said relaxation time of said

5 hyperpolarized noble gas is longer than said relaxation time of said noble
6 gas in said physiological fluid; and

7 (b) contacting said physiological fluid with said intermediate solution.

1 36. A method for measuring a signal transferred from a hyperpolarized noble
2 gas atom to a non-noble gas NMR active nucleus, comprising:

- 3 (a) contacting a non-noble gas NMR active nucleus with a hyperpolarized noble
4 gas atom;
- 5 (b) applying radiofrequency energy to said non-noble gas NMR active
6 nucleus; and
- 7 (c) measuring said signal transferred from said hyperpolarized noble
8 gas atom to said non-noble gas NMR active nucleus using
9 nuclear magnetic resonance spectroscopy, magnetic resonance imaging, or
10 both.

1 37. A pulse sequence for heteronuclear difference spin polarization induced
2 nuclear Overhauser effect (SPINOE) NMR of a system comprising a noble gas atom and
3 a non-noble gas NMR active nucleus, comprising:

- 4 (a) a non-noble gas NMR active nucleus $\pi/2$ pulse
- 5 (b) a non-noble gas NMR active nucleus π pulse applied simultaneously
6 with application of a noble gas π pulse; and
- 7 (c) a non-noble gas NMR active nucleus $\pi/2$ pulse.

1 38. An apparatus for preparing a solution of a hyperpolarized noble gas,
2 said apparatus comprising:

3 a vessel for receiving a fluid;
4 a reservoir for receiving said hyperpolarized noble gas, the reservoir
5 communicating through a first shutoff valve with said vessel, said reservoir being shaped
6 to allow said reservoir to be cooled independently of said vessel;
7 a gas inlet port communicating through a second shutoff valve with said reservoir; and
8 a means for withdrawing said fluid from said vessel independently of said first
9 shutoff valve and said second shutoff valve.

1 39. An apparatus according to claim 38 further comprising:
2 a means for freezing said hyperpolarized noble gas.

1 40. An apparatus according to claim 38 further comprising:
2 a means for applying a magnetic field to said reservoir for receiving said
3 hyperpolarized noble gas.

1/22

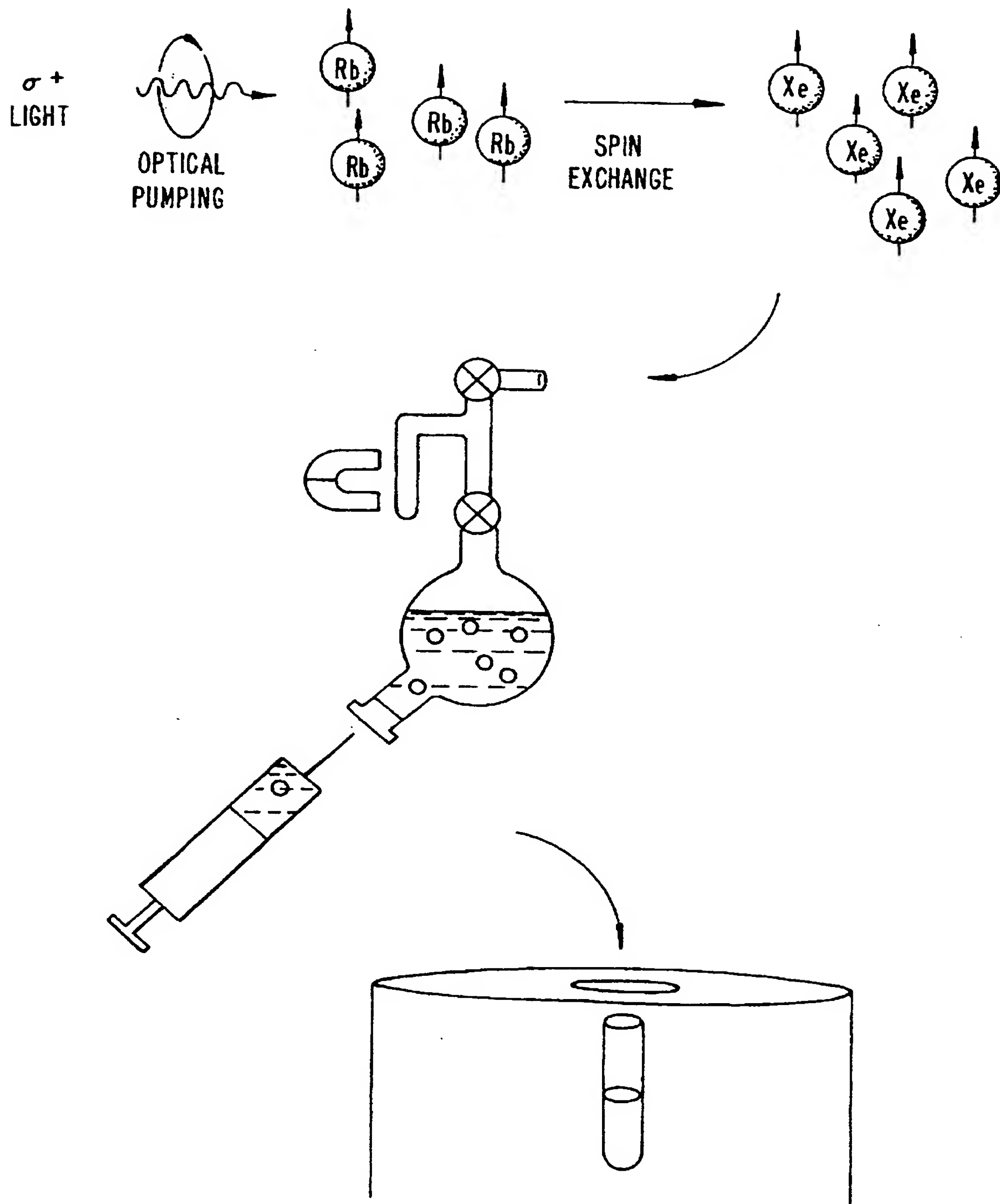


FIG. 1.

SUBSTITUTE SHEET (RULE 26)

2/22

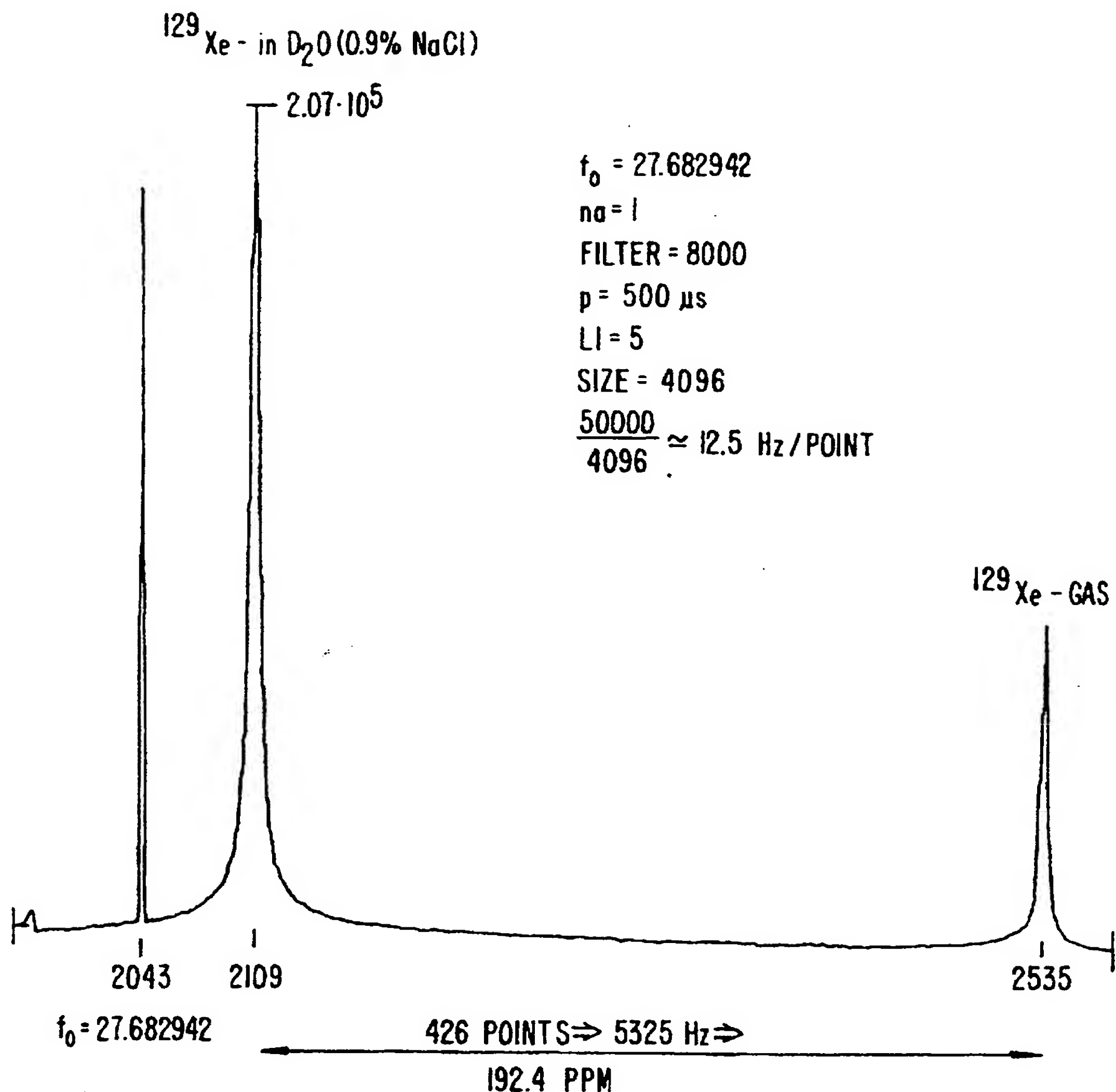


FIG. 2.

3/22

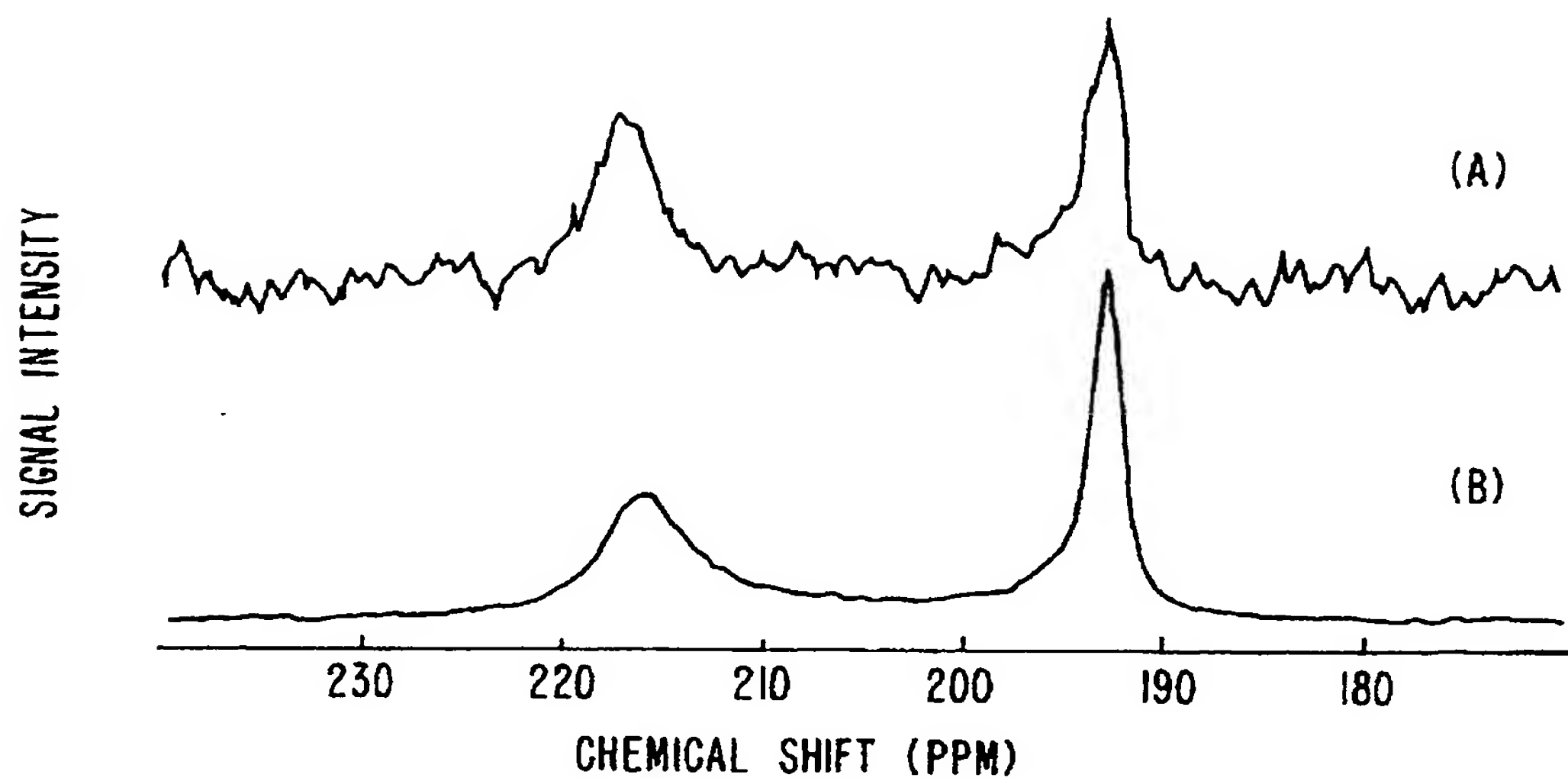


FIG. 3.

4/22

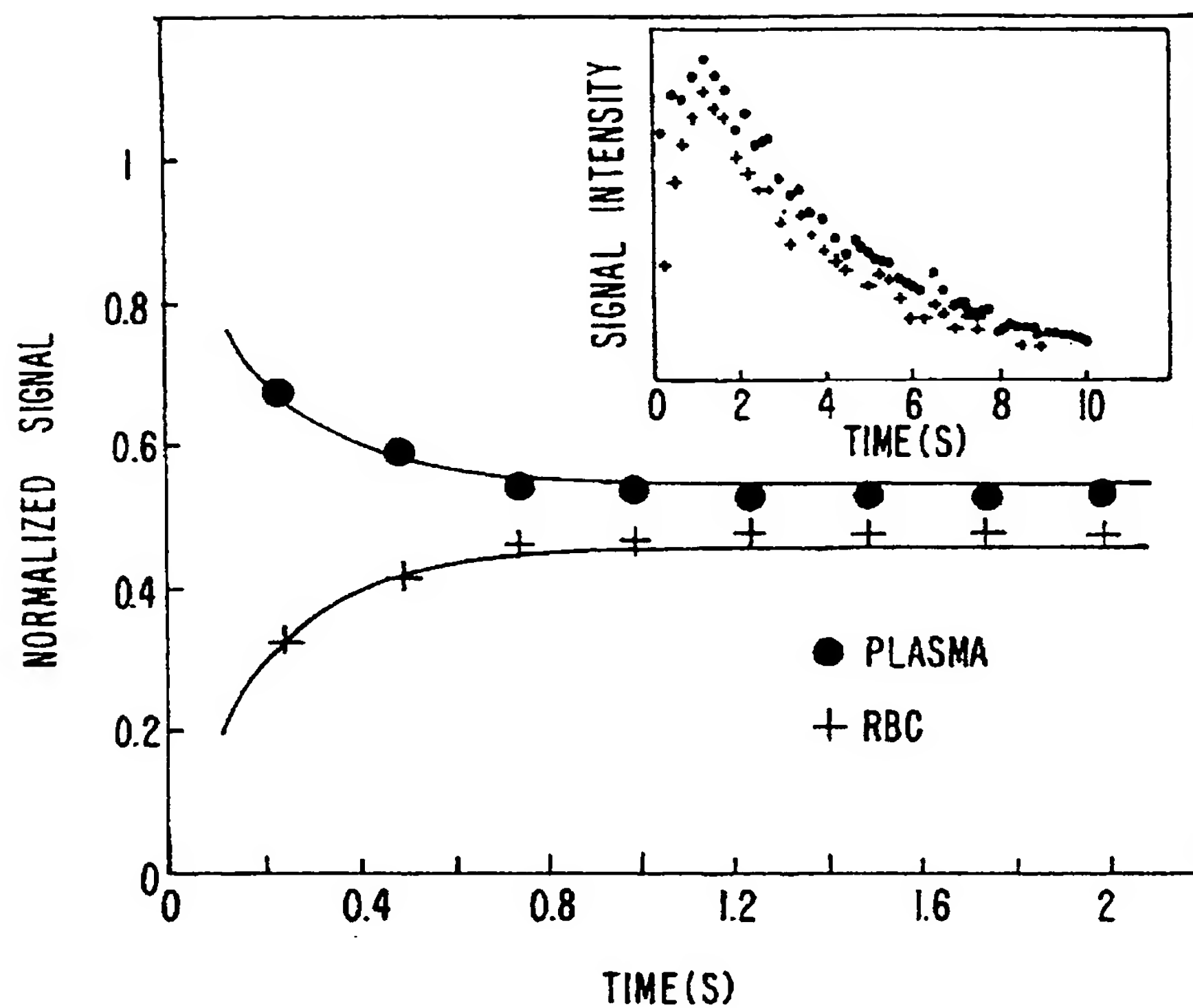


FIG. 4.

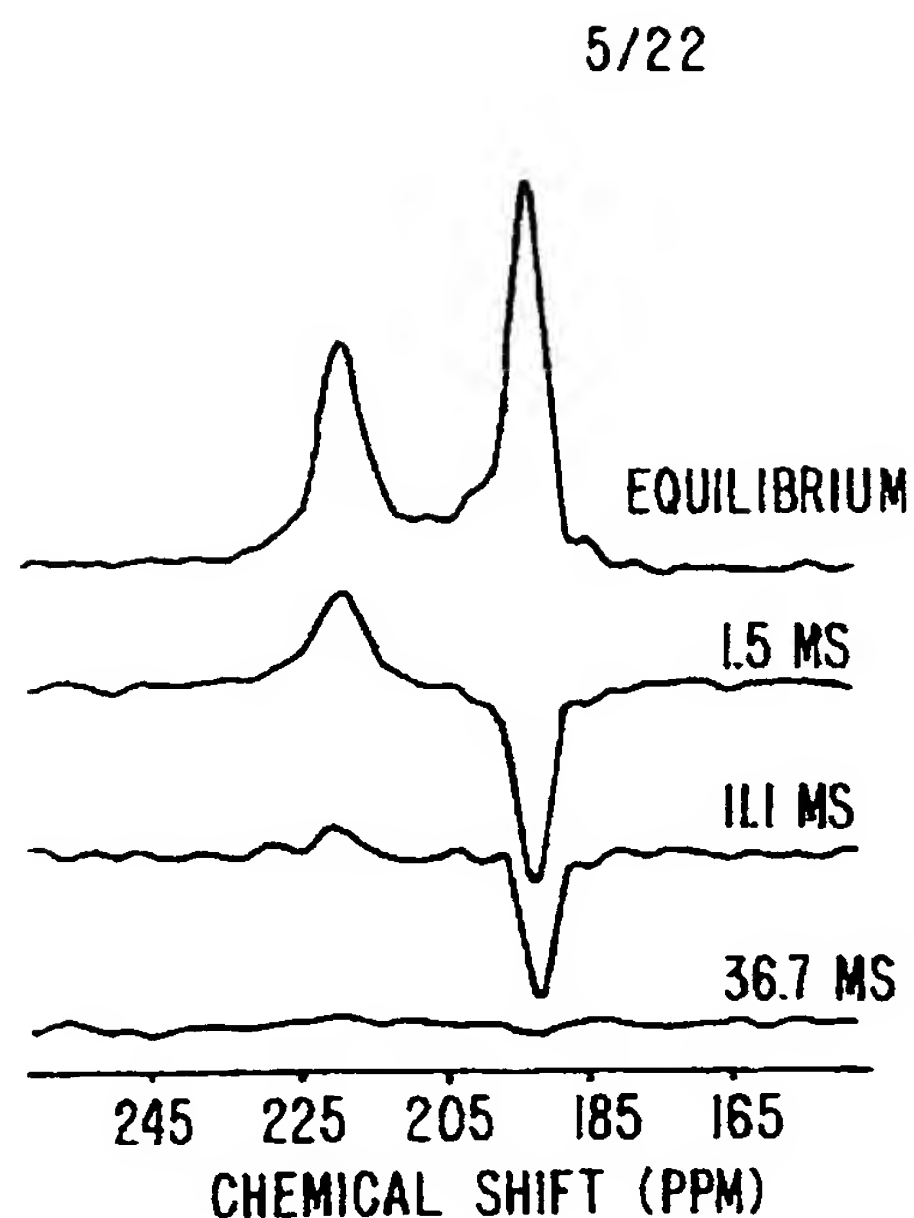


FIG. 5A.

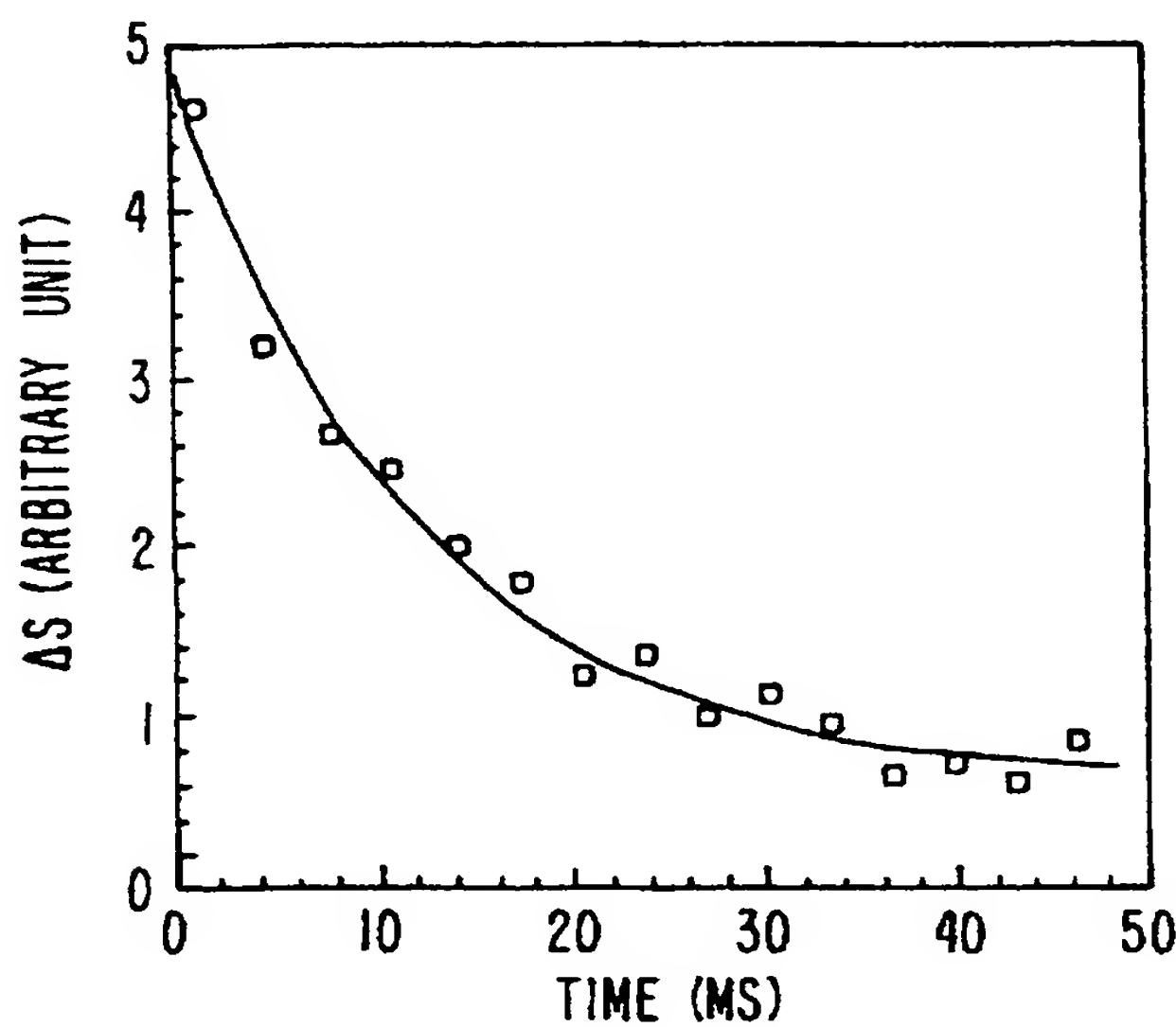


FIG. 5B.

6/22

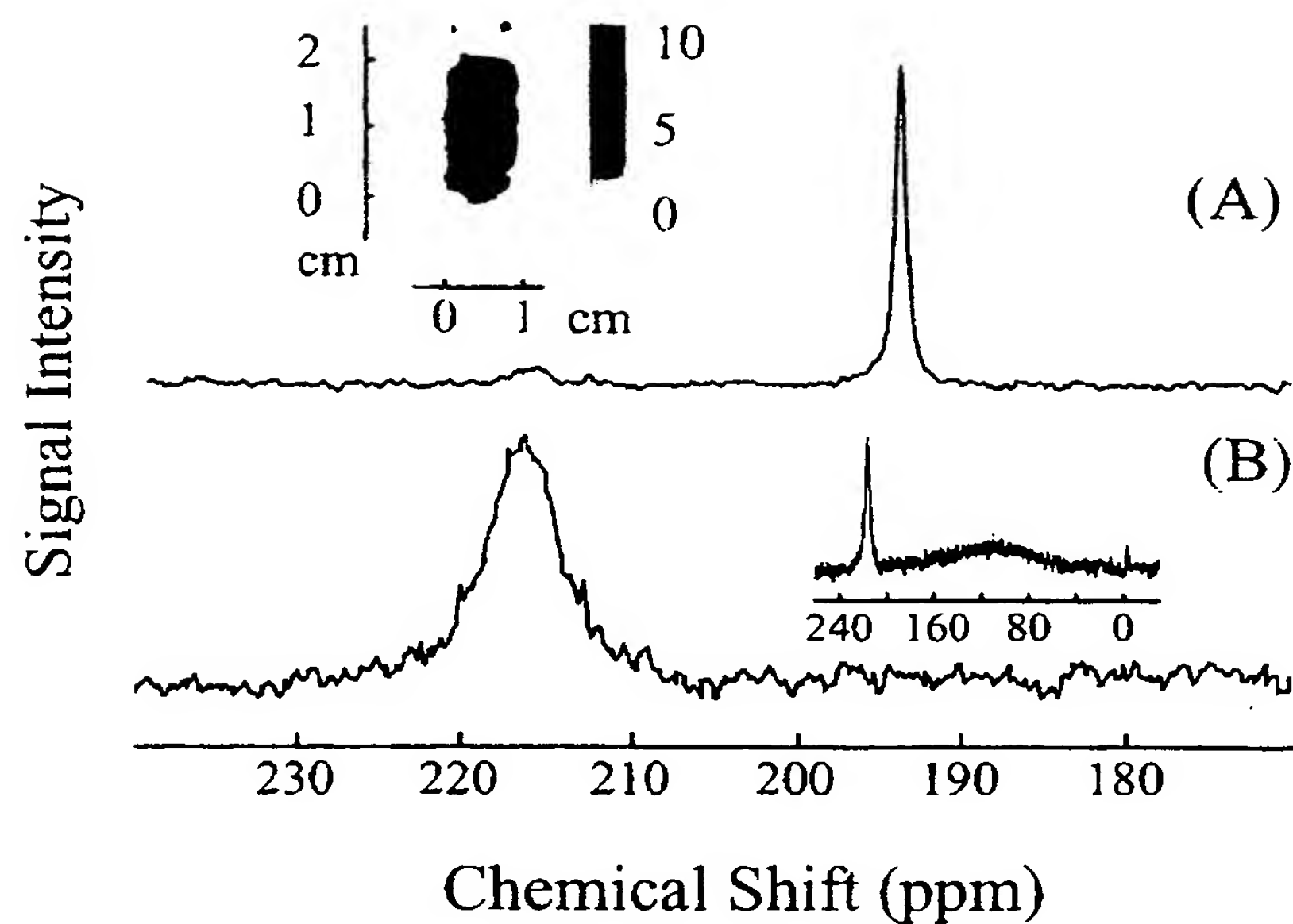


FIG. 6.

^{129}Xe MRI in Blood

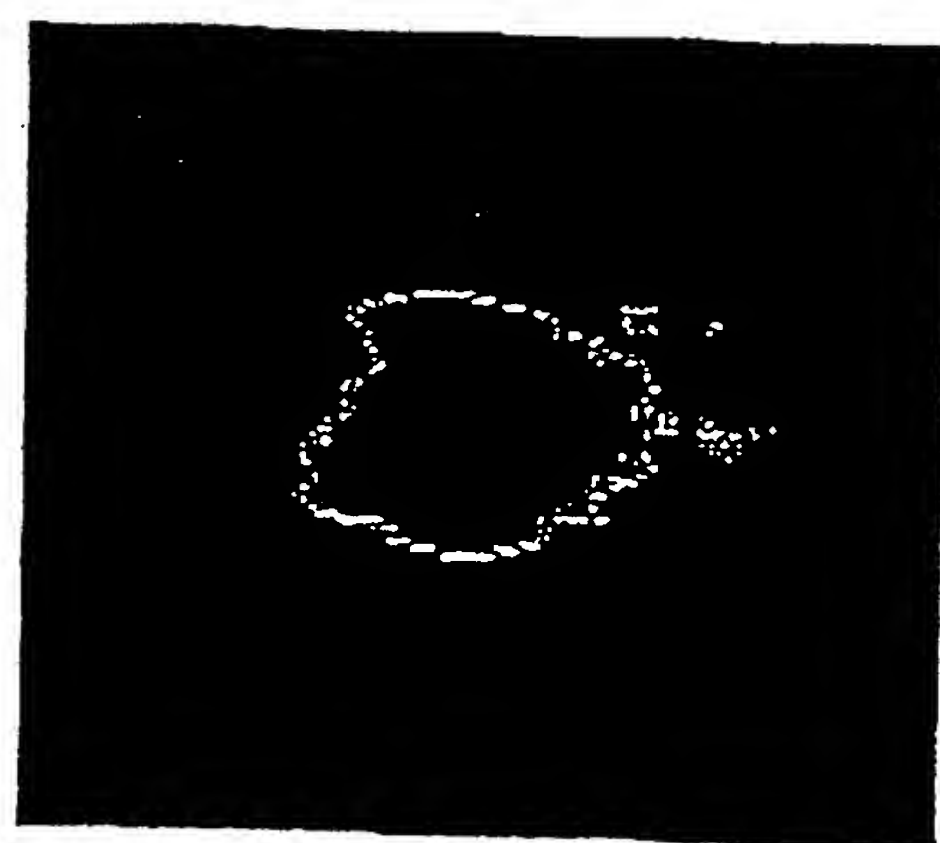


FIG. 7

8/22

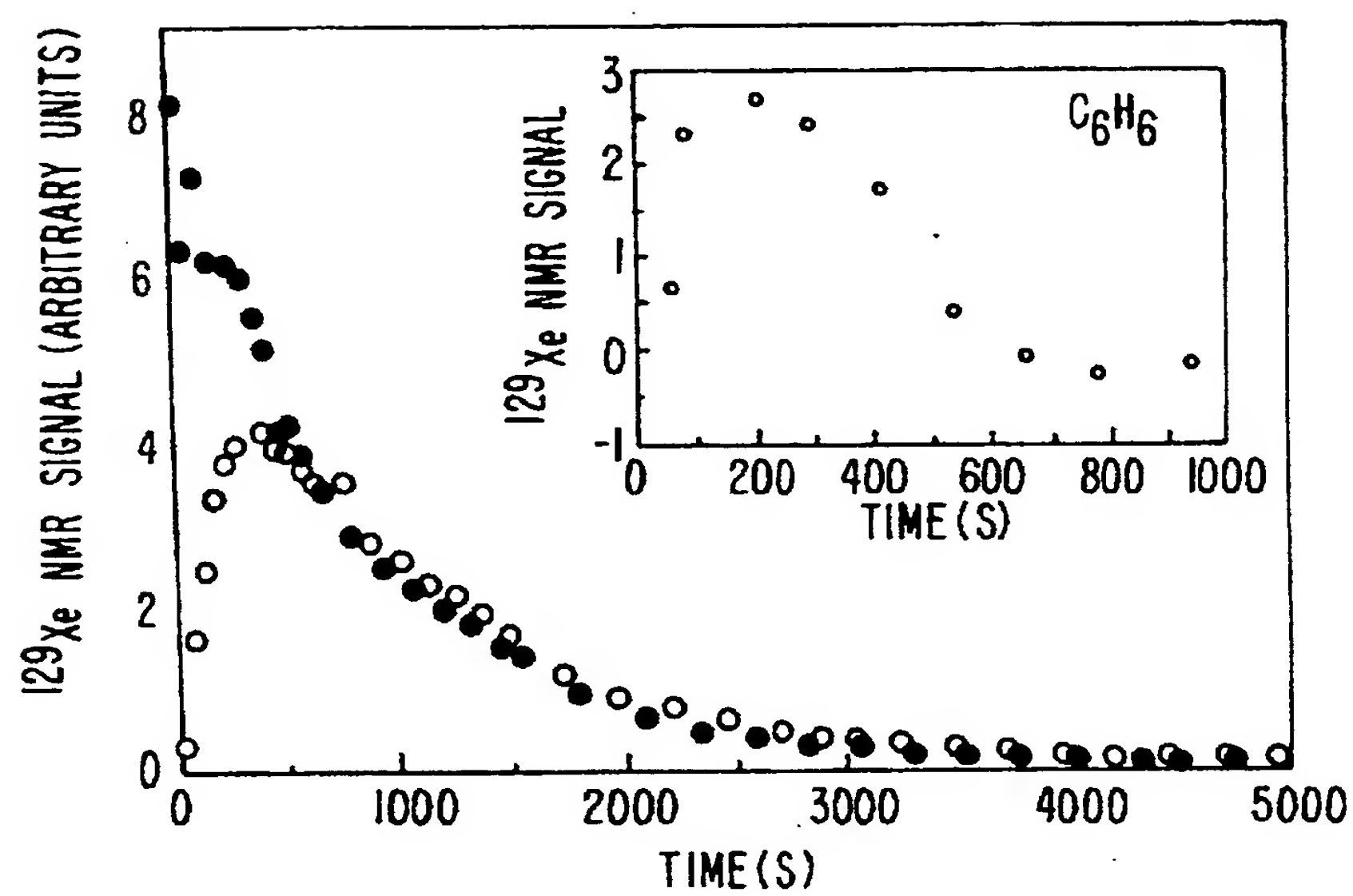


FIG. 8.

9/22

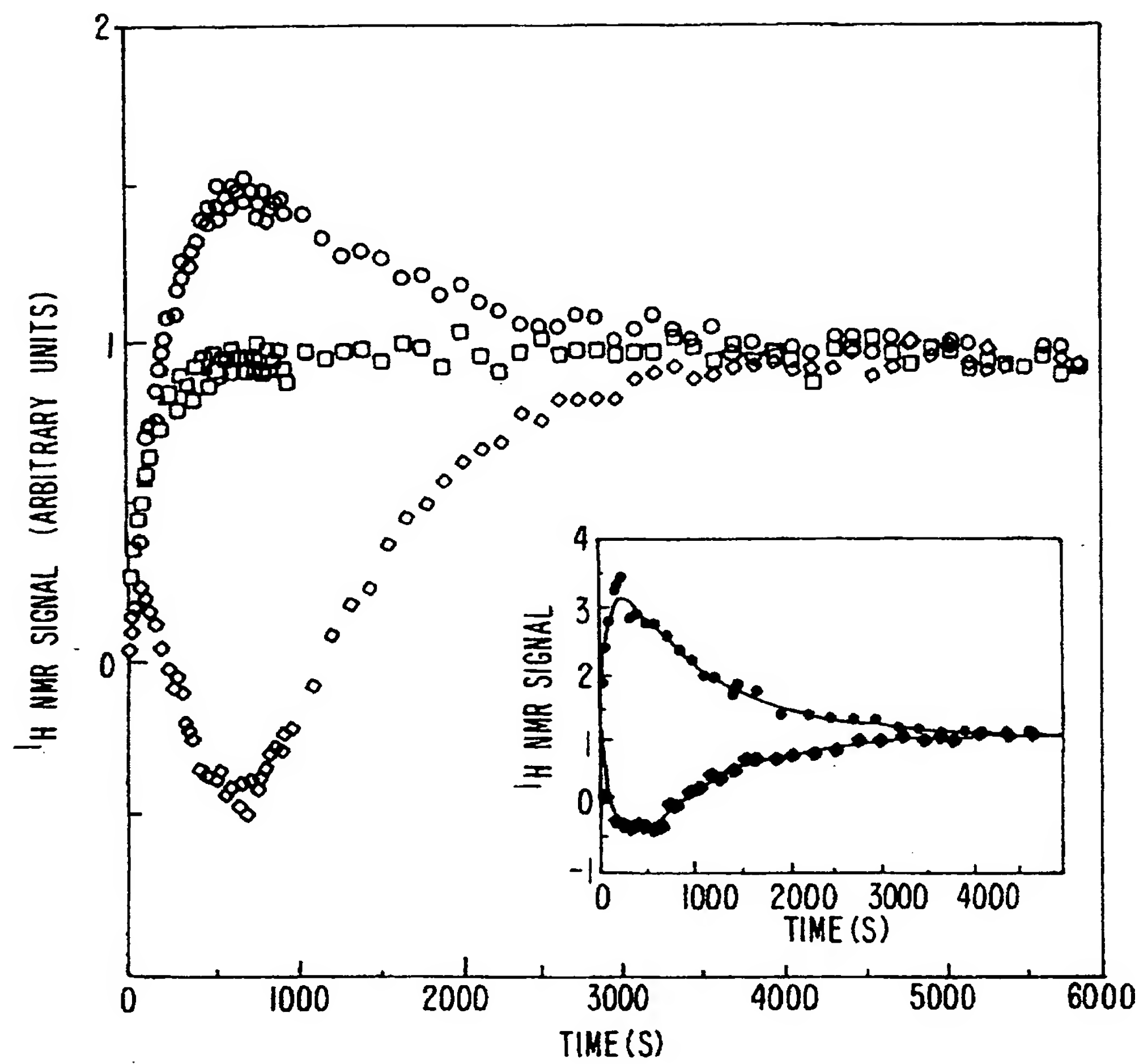


FIG. 9.

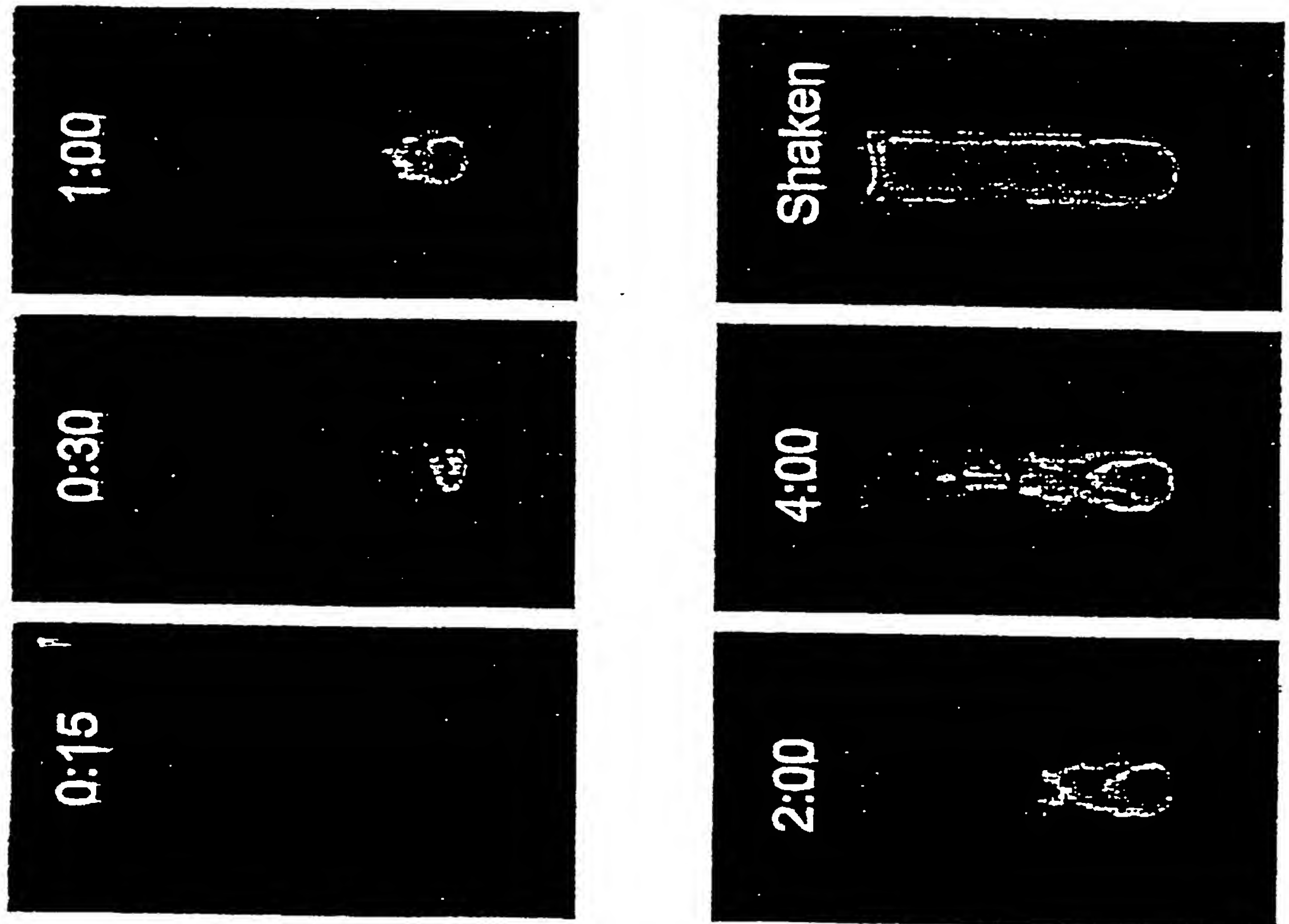


FIG. 10

II/22

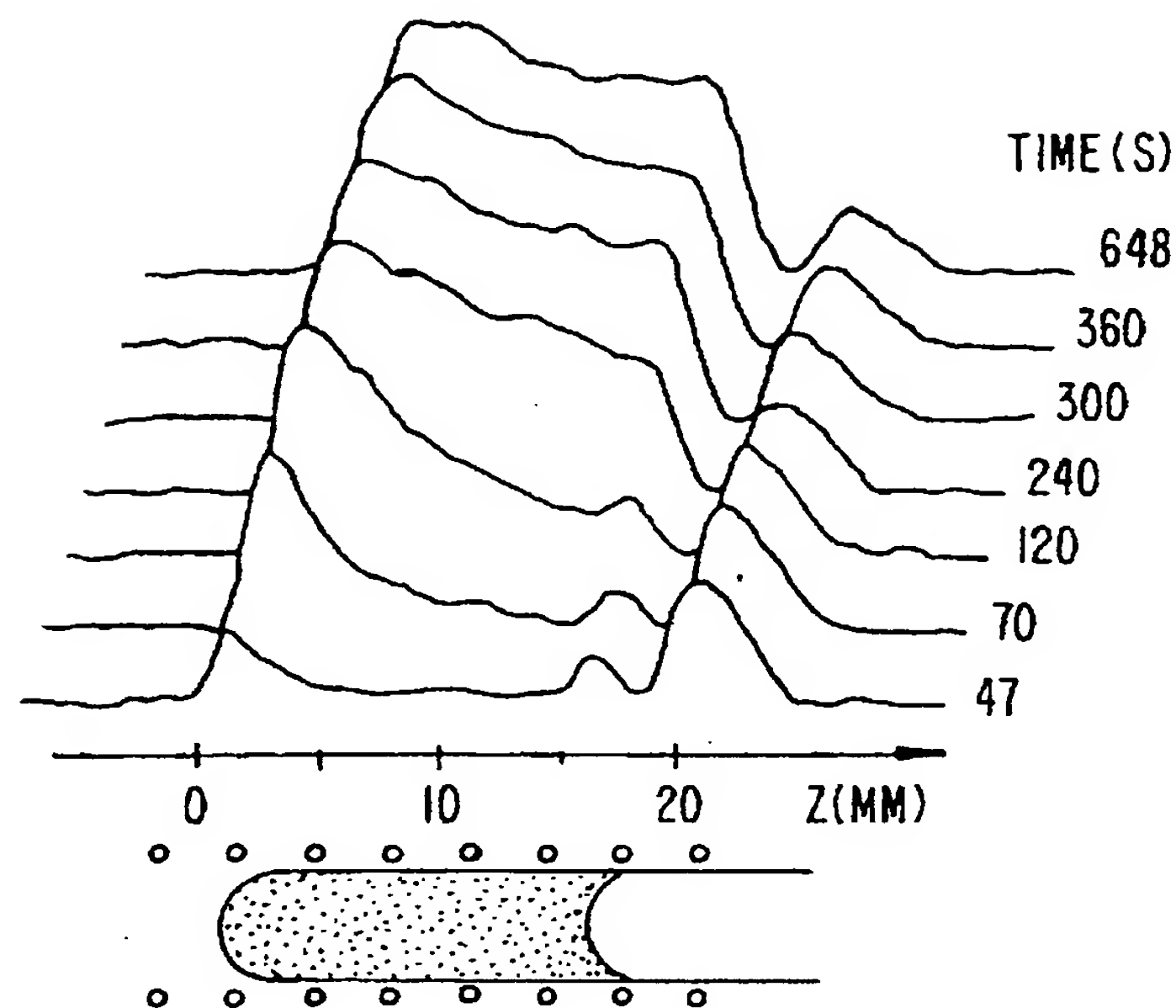


FIG. II.

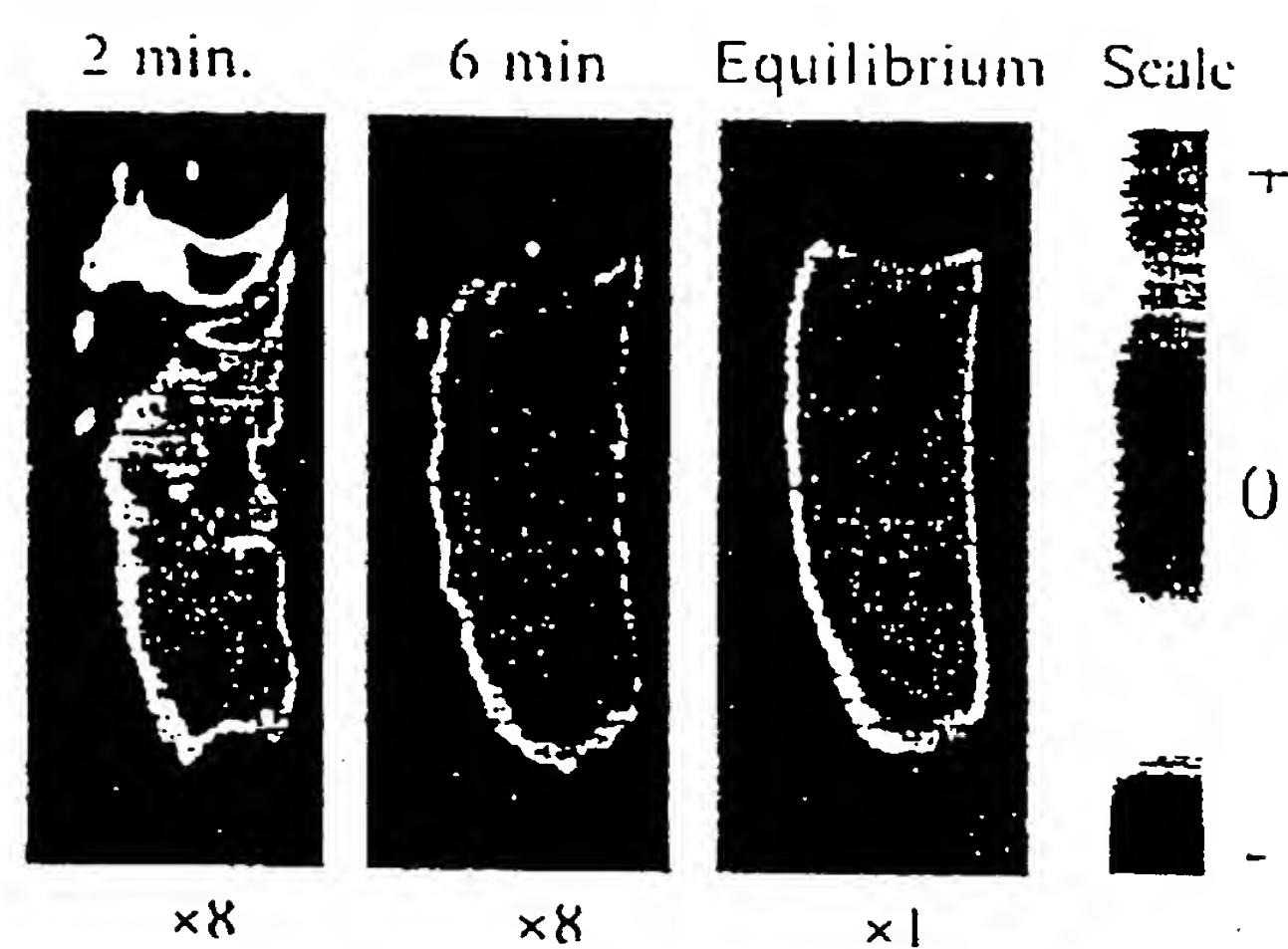
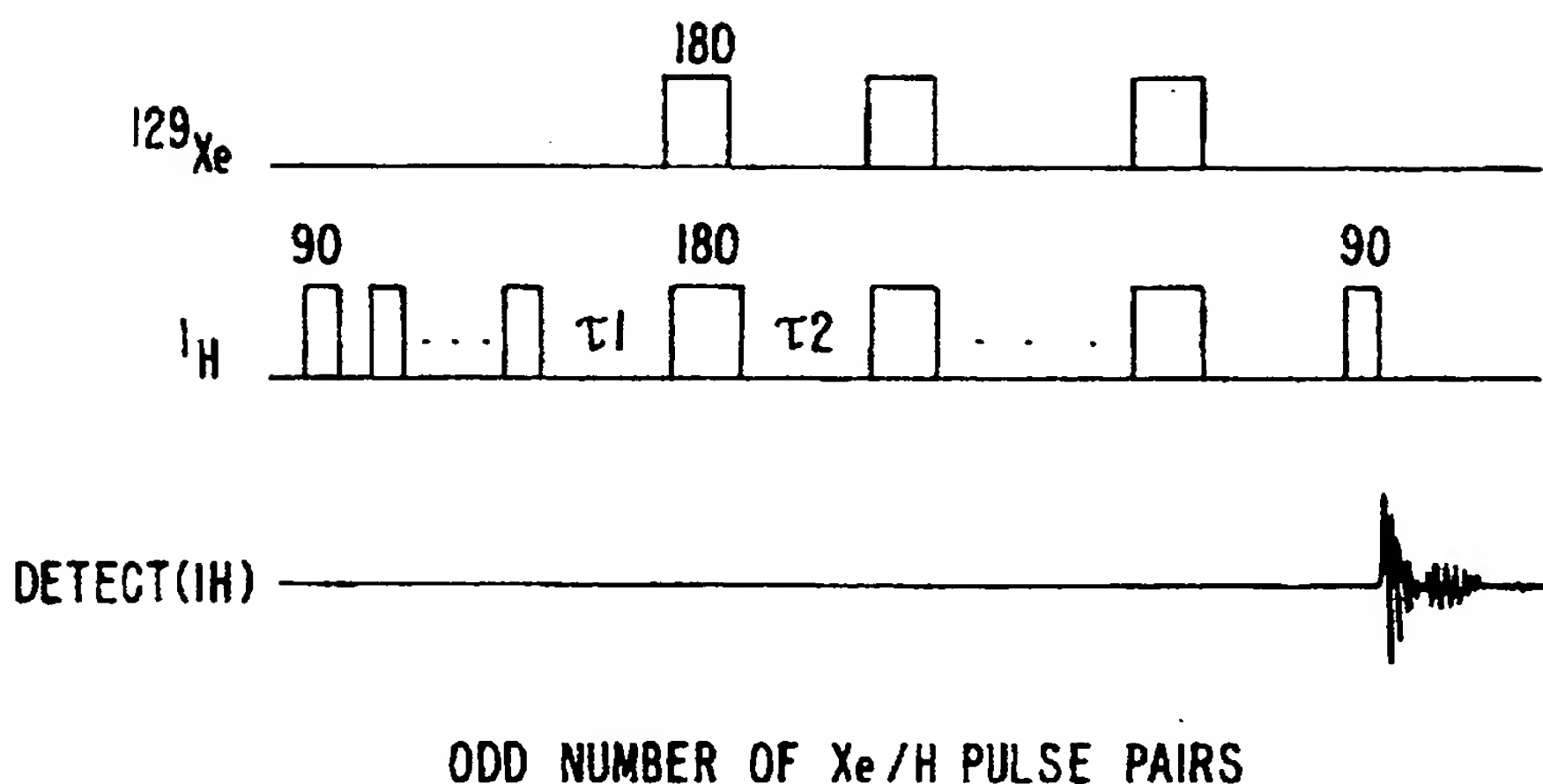


FIG. 12

13/22



ODD NUMBER OF Xe/H PULSE PAIRS

FIG. 13.

14/22

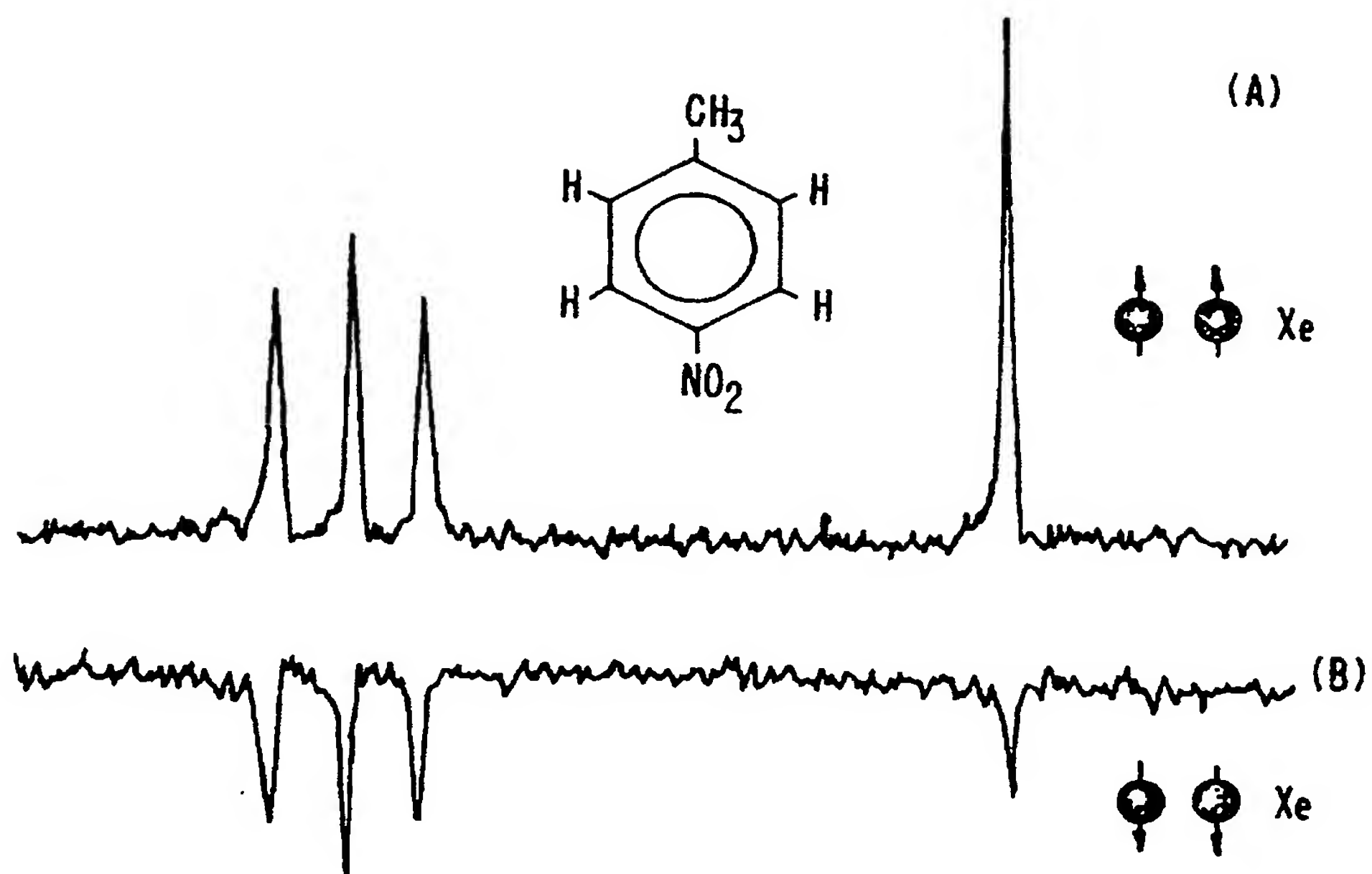


FIG. 14.

15/22

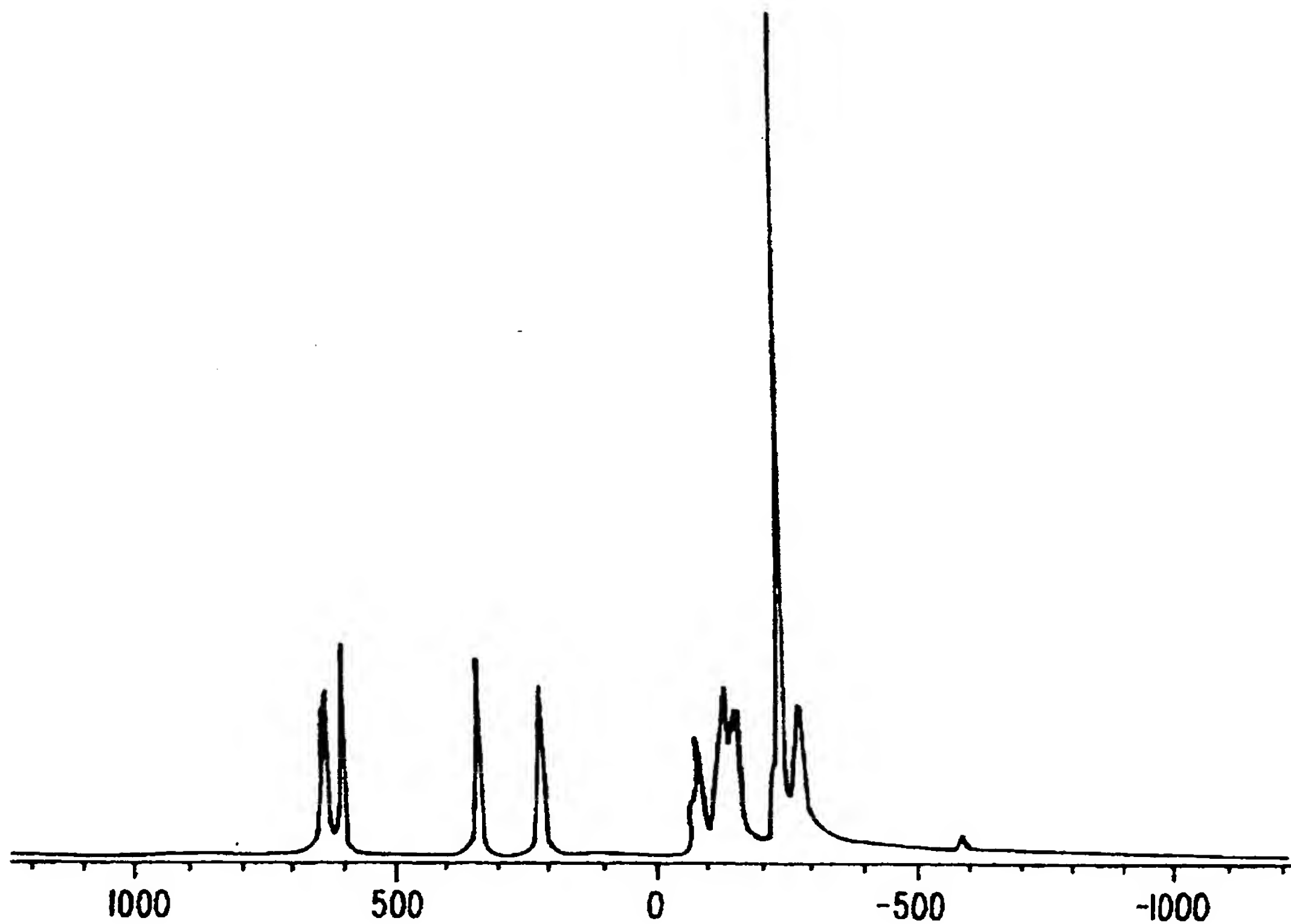


FIG. 15.

16/22

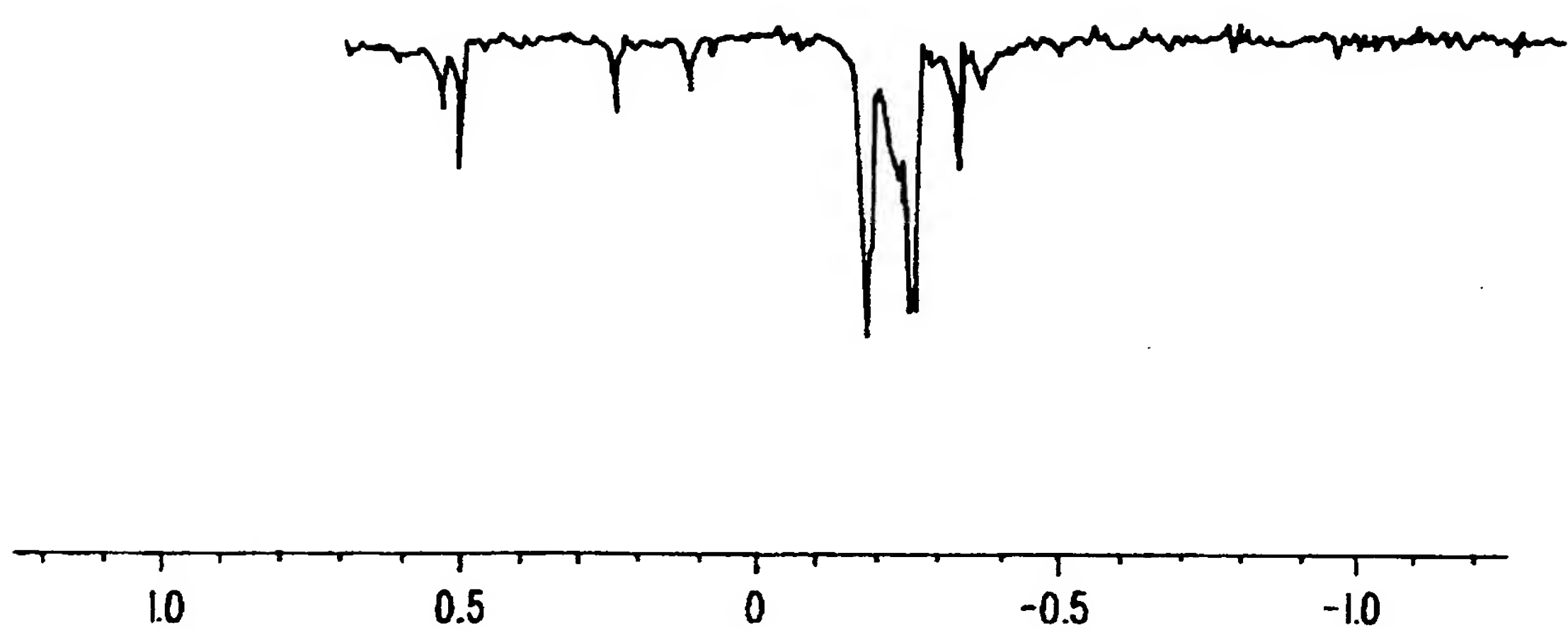


FIG. 16.

17/22

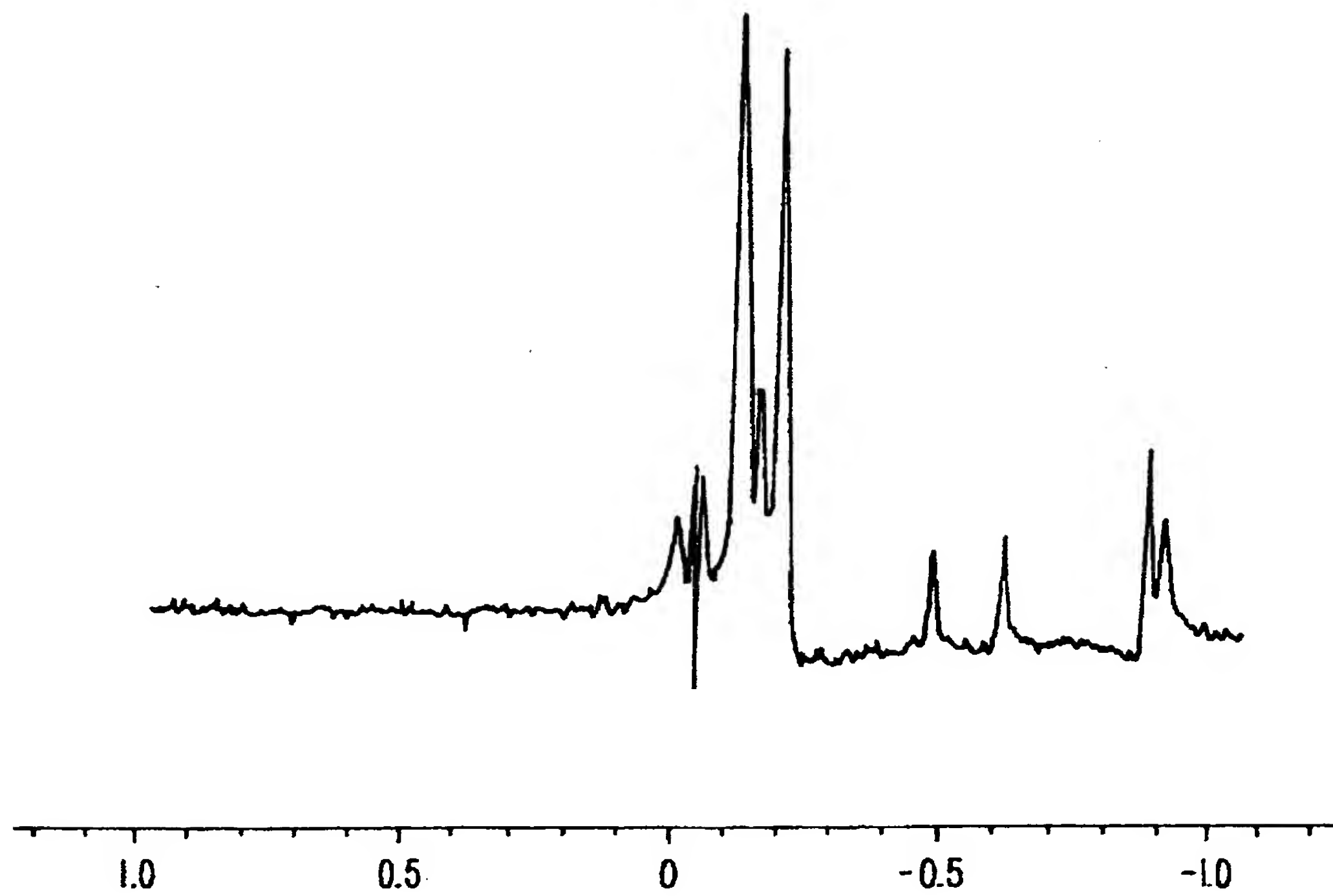


FIG. 17.

18/22

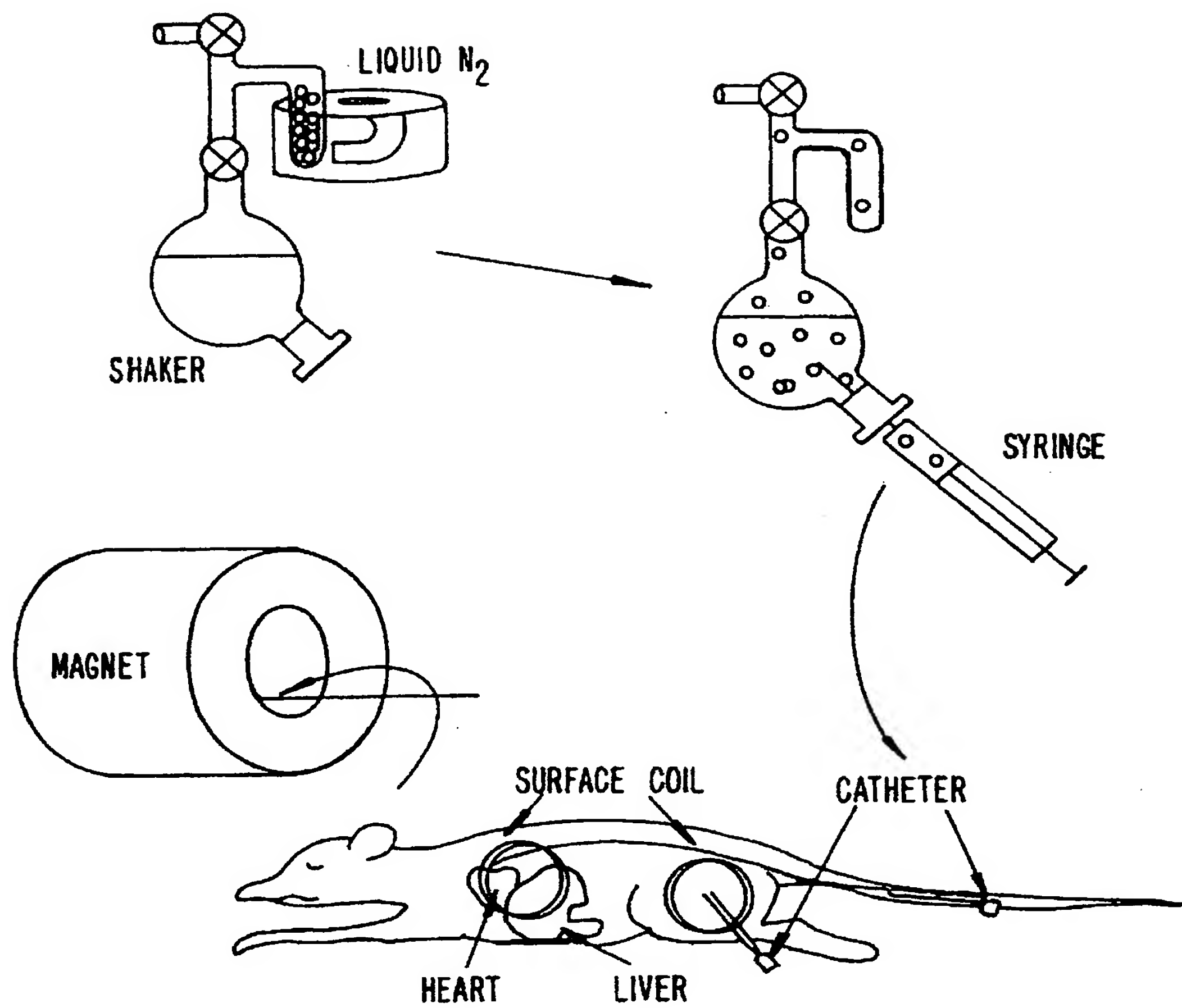


FIG. 18.

SUBSTITUTE SHEET (RULE 26)

19/22

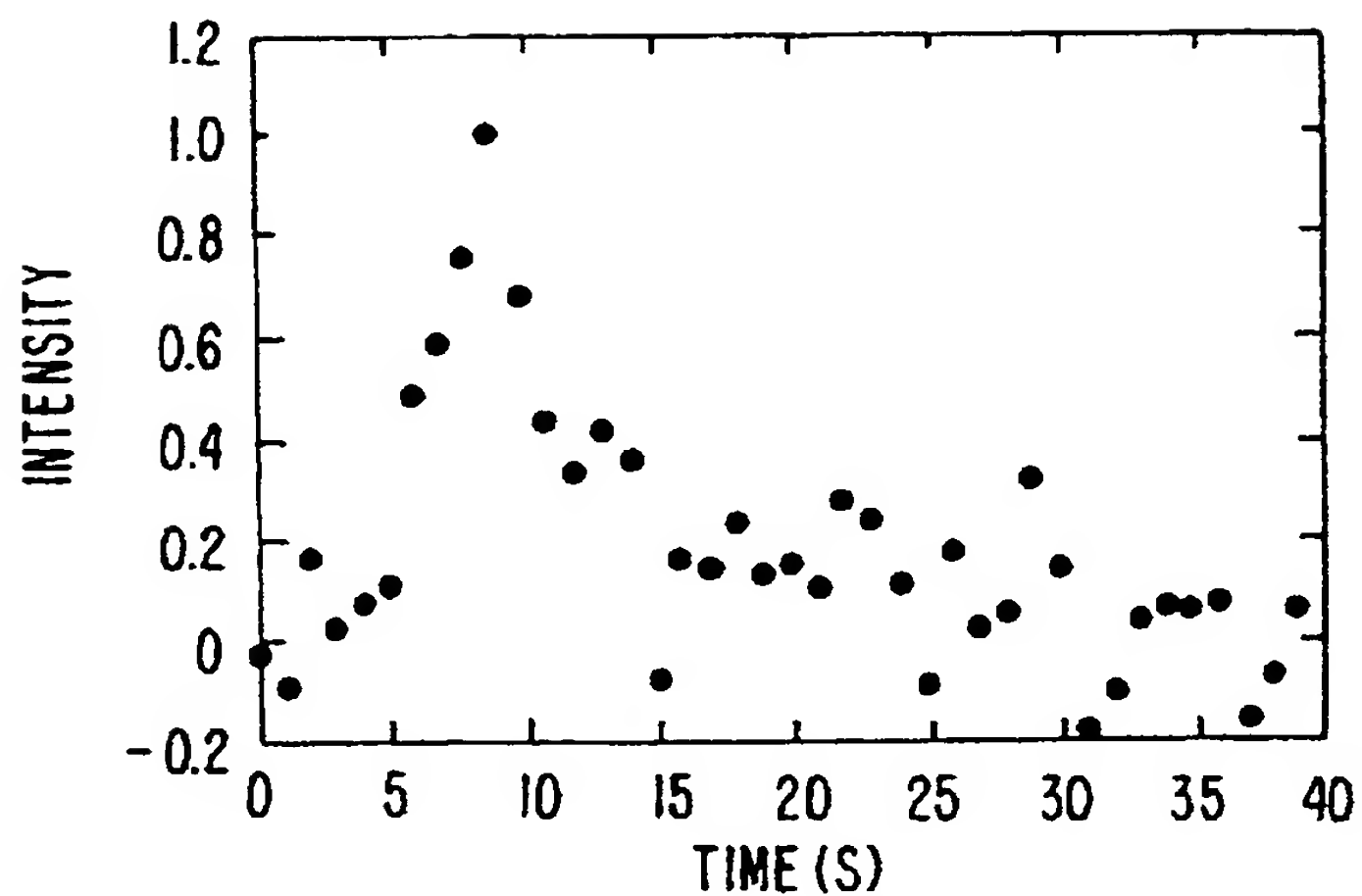


FIG. 19A.

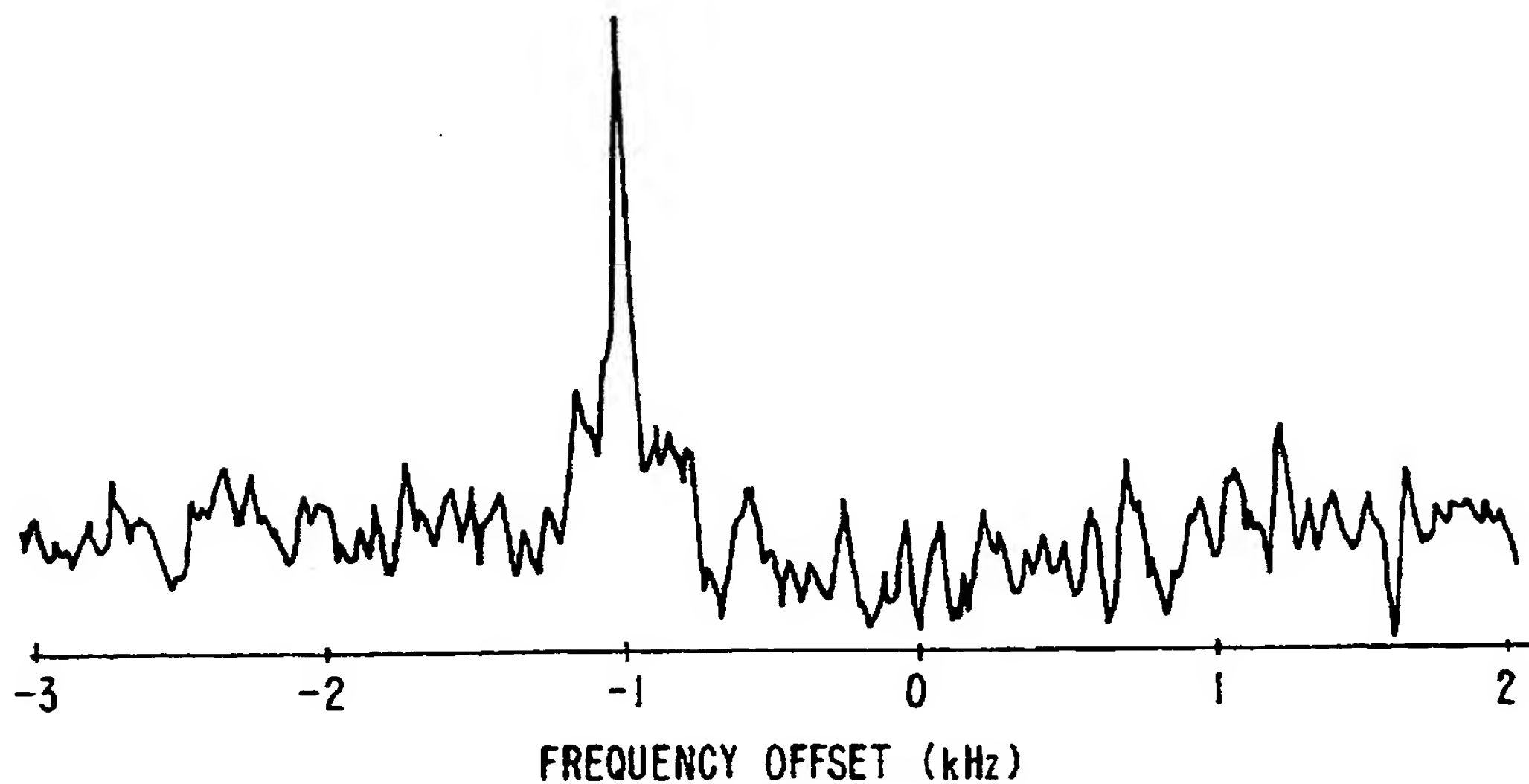


FIG. 19B.

20/22

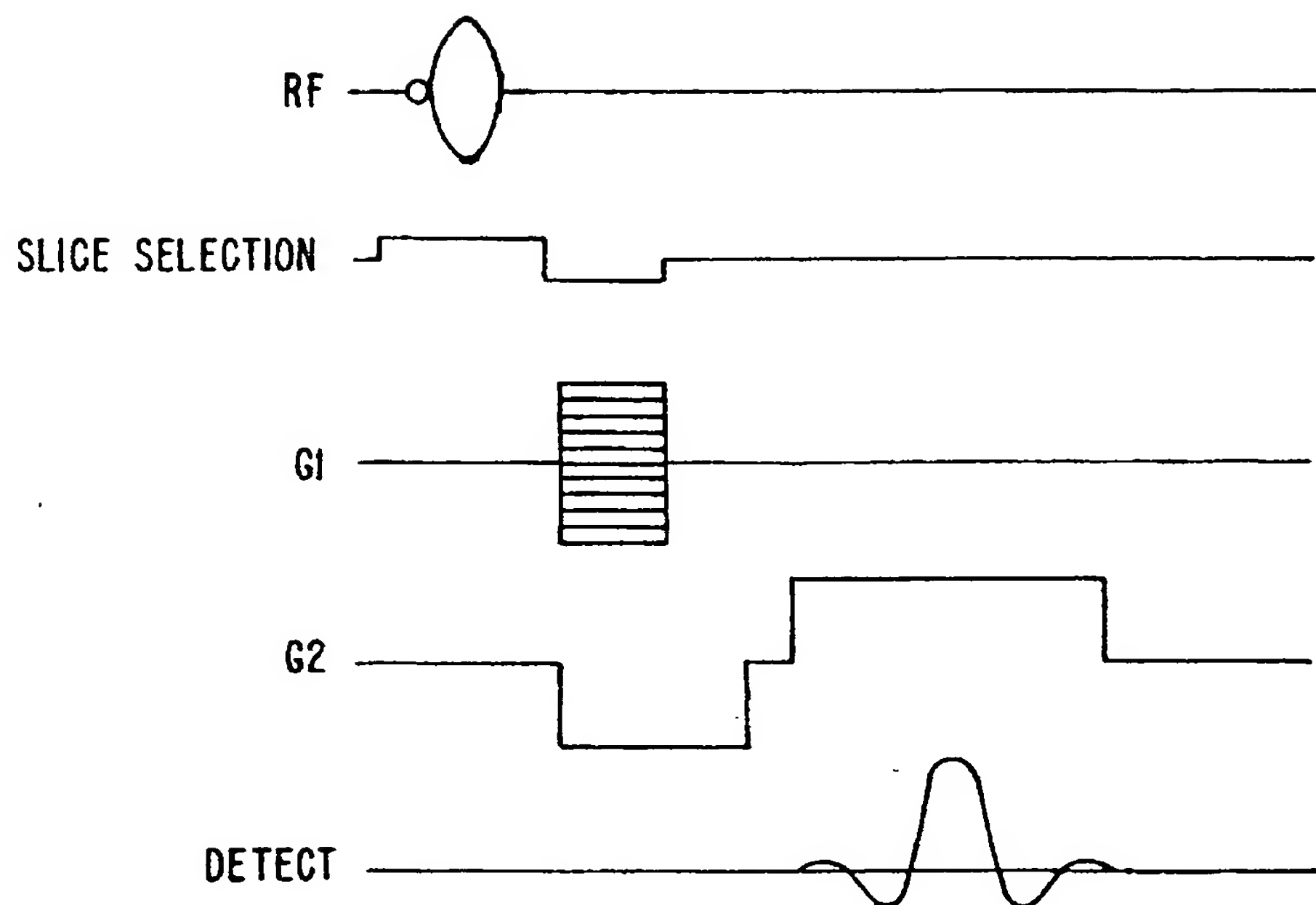


FIG. 20.

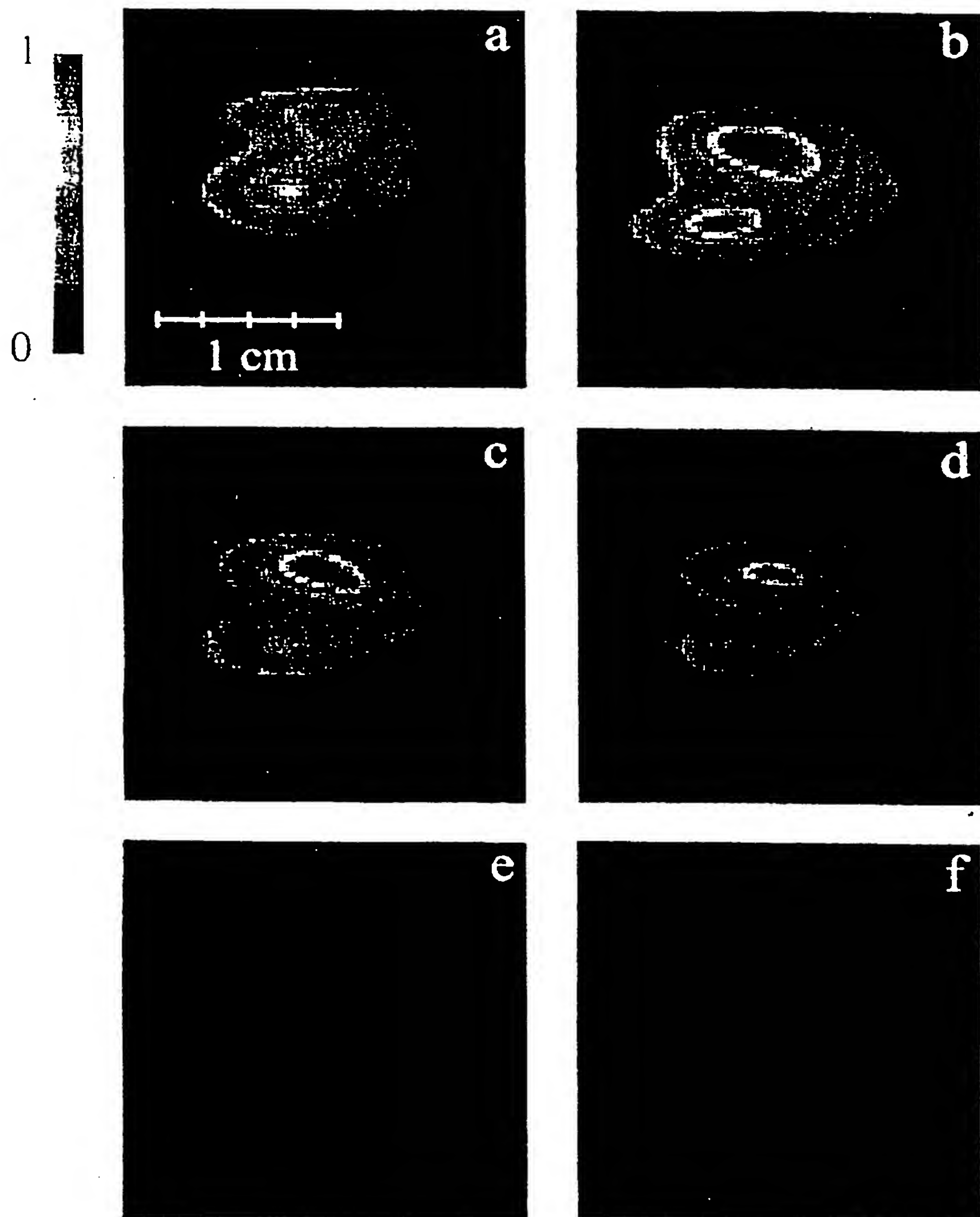


FIG. 21

22/22

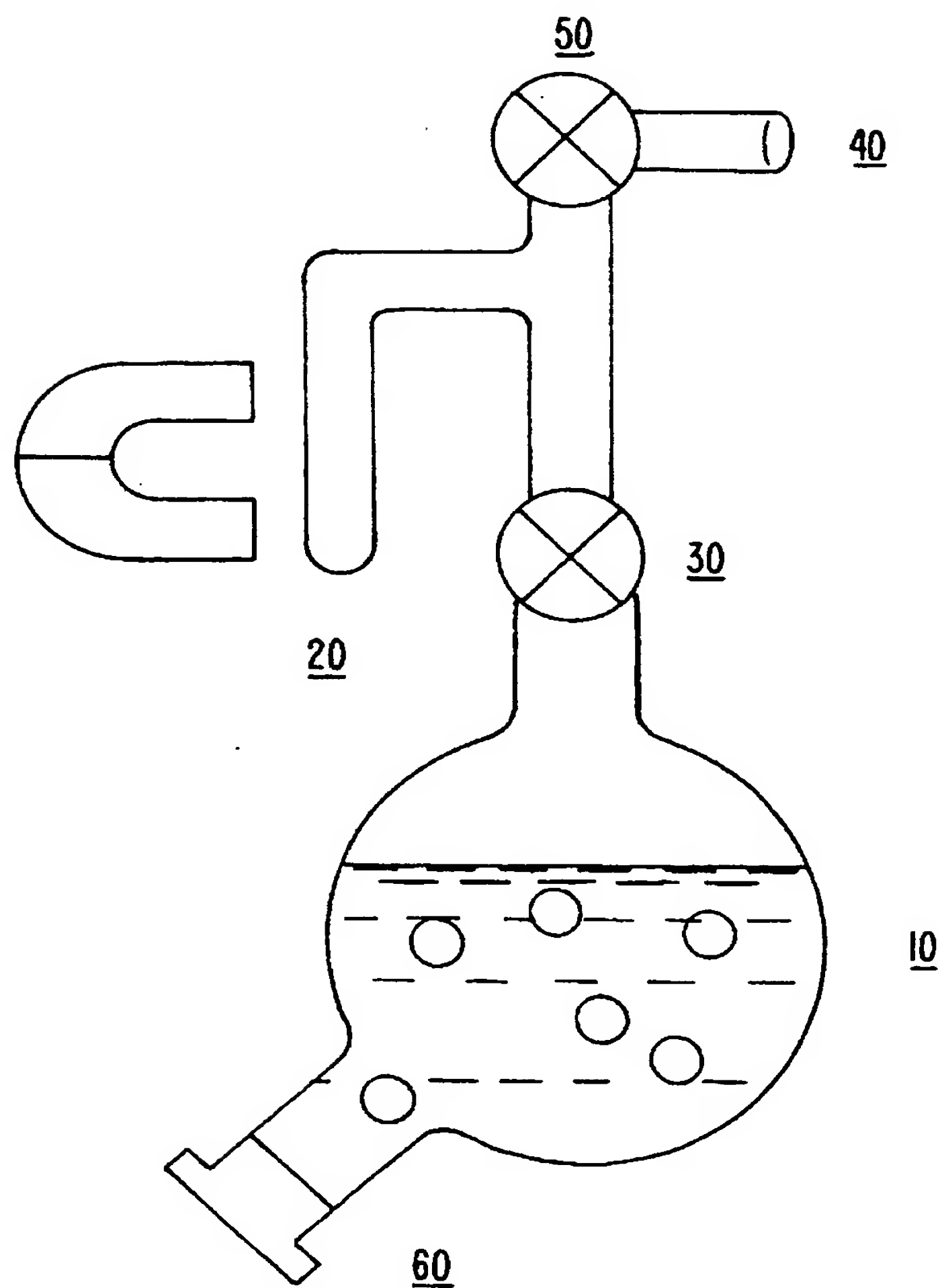


FIG. 22.

INTERNATIONAL SEARCH REPORT

International Application No
PCT/US 97/05166

A. CLASSIFICATION OF SUBJECT MATTER
IPC 6 G01R33/28

According to International Patent Classification (IPC) or to both national classification and IPC

B. FIELDS SEARCHED

Minimum documentation searched (classification system followed by classification symbols)
IPC 6 G01R A61K

Documentation searched other than minimum documentation to the extent that such documents are included in the fields searched

Electronic data base consulted during the international search (name of data base and, where practical, search terms used)

C. DOCUMENTS CONSIDERED TO BE RELEVANT

Category ^a	Citation of document, with indication, where appropriate, of the relevant passages	Relevant to claim No.
X	WO 95 27438 A (THE RESEARCH FOUNDATION OG STATE UNIVERSITY OF NEW YORK) 19 October 1995 see page 6, line 12 - page 9, line 36 see page 14, line 6 - page 23, line 33 see page 25, line 6 - line 34 see page 26, line 18 - page 27, line 4 ---	1-35, 38-40
X	JOURNAL OF MAGNETIC RESONANCE, SERIES A, vol. 115, 1995, pages 127-130, XP000519715 Y.-Q. SONG ET AL.: "Spin-Polarized ¹²⁹ Xe Gas Imaging of Materials" cited in the application	3-35
A	see the whole document ---	1, 2, 36, 37 -/-

Further documents are listed in the continuation of box C.

Patent family members are listed in annex.

^a Special categories of cited documents :

- "A" document defining the general state of the art which is not considered to be of particular relevance
- "E" earlier document but published on or after the international filing date
- "L" document which may throw doubts on priority claim(s) or which is cited to establish the publication date of another citation or other special reason (as specified)
- "O" document referring to an oral disclosure, use, exhibition or other means
- "P" document published prior to the international filing date but later than the priority date claimed

- "T" later document published after the international filing date or priority date and not in conflict with the application but cited to understand the principle or theory underlying the invention
- "X" document of particular relevance; the claimed invention cannot be considered novel or cannot be considered to involve an inventive step when the document is taken alone
- "Y" document of particular relevance; the claimed invention cannot be considered to involve an inventive step when the document is combined with one or more other such documents, such combination being obvious to a person skilled in the art.
- "&" document member of the same patent family

1

Date of the actual completion of the international search

14 July 1997

Date of mailing of the international search report

28/07/1997

Name and mailing address of the ISA

European Patent Office, P.B. 5818 Patentlaan 2
NL - 2280 HV Rijswijk
Tel. (+31-70) 340-2040, Tx. 31 651 epo nl.
Fax: (+31-70) 340-3016

Authorized officer

Volmer, W

INTERNATIONAL SEARCH REPORTInternational Application No
PCT/US 97/05166**C. DOCUMENTS CONSIDERED TO BE RELEVANT**

Category	Character of document, with indication, where appropriate, of the relevant passages	Relevant to claim No.
X	MAGNETIC RESONANCE IN MEDICINE, vol. 33, 1995, pages 271-275, XP002034982 H. MIDDLETON ET AL.: "MR Imaging with Hyperpolarized 3He Gas" cited in the application	3-35
A	see the whole document -----	1, 2, 36, 37

INTERNATIONAL SEARCH REPORT

Information on patent family members

International Application No
PCT/US 97/05166

Patent document cited in search report	Publication date	Patent family member(s)	Publication date
WO 9527438 A	19-10-95	US 5545396 A AU 2278795 A CA 2183740 A EP 0754009 A	13-08-96 30-10-95 19-10-95 22-01-97

**This Page is Inserted by IFW Indexing and Scanning
Operations and is not part of the Official Record**

BEST AVAILABLE IMAGES

Defective images within this document are accurate representations of the original documents submitted by the applicant.

Defects in the images include but are not limited to the items checked:

- BLACK BORDERS**
- IMAGE CUT OFF AT TOP, BOTTOM OR SIDES**
- FADED TEXT OR DRAWING**
- BLURRED OR ILLEGIBLE TEXT OR DRAWING**
- SKEWED/SLANTED IMAGES**
- COLOR OR BLACK AND WHITE PHOTOGRAPHS**
- GRAY SCALE DOCUMENTS**
- LINES OR MARKS ON ORIGINAL DOCUMENT**
- REFERENCE(S) OR EXHIBIT(S) SUBMITTED ARE POOR QUALITY**
- OTHER:** _____

IMAGES ARE BEST AVAILABLE COPY.

As rescanning these documents will not correct the image problems checked, please do not report these problems to the IFW Image Problem Mailbox.